Jouni Pyykönen

Computational simulation of aerosol behaviour

TECHNICAL RESEARCH CENTRE OF FINLAND ESPOO 2002

VTT PUBLICATIONS 461

Computational simulation of aerosol behaviour

Jouni Pyykönen

VTT Processes

Dissertation for the degree of Doctor of Science in Technology to be presented with due permission for public examination and debate in Auditorium E at Helsinki University of Technology (Espoo, Finland) on the 22nd of March, 2002 at 12 o'clock noon

TECHNICAL RESEARCH CENTRE OF FINLAND
ESPOO 2002

ISBN 951–38–5977–0 (soft back ed.)
ISSN 1235–0621 (soft back ed.)

ISBN 951–38–5978–9 (URL:http://www.inf.vtt.fi/pdf/)
ISSN 1455–0849 (URL:http://www.inf.vtt.fi/pdf/)

JULKAISIJA – UTGIVARE – PUBLISHER

Valtion teknillinen tutkimuskeskus (VTT), Vuorimiehentie 5, PL 2000, 02044 VTT
puh. vaihde (09) 4561, faksi (09) 456 4374

Statens tekniska forskningscentral (VTT), Bergsmansvägen 5, PB 2000, 02044 VTT
tel. växel (09) 4561, fax (09) 456 4374

Technical Research Centre of Finland (VTT), Vuorimiehentie 5, P.O.Box 2000, FIN–02044 VTT, Finland
phone internat. + 358 9 4561, fax + 358 9 456 4374

VTT Prosessit, Prosessit ja ympäristö, Biologinkuja 7, PL 1401, 02044 VTT
puh. vaihde (09) 4561, faksi (09) 456 7021

VTT Processer, Processer och miljö, Biologgränden 7, PB 1401, 02044 VTT
tel. växel (09) 4561, fax (09) 456 7021

VTT Processes, Processes and Environment,
Biologinkuja 7, P.O.Box 1401, FIN–02044 VTT, Finland
phone internat. + 358 9 4561, fax + 358 9 456 7021

Technical editing Maini Manninen

Otamedia Oy, Espoo 2002

Pyykönen, Jouni. Computational simulation of aerosol behaviour. Espoo 2002. Technical Research Centre of Finland, VTT Publications 461. 70 p. + app. 154 p.

Keywords aerosols, aerosol formation, deposition, modelling, population balances, computational fluid dynamics, laminar flow reactors, combustion processes, fly ash, recovery boilers, boundary layers

Abstract

In this thesis, computational methods have been developed for the simulation of aerosol dynamics and transport. Two different coupled aerosol-computational fluid dynamics (CFD) models are discussed. One is a full Eulerian model and the other is a boundary layer-type streamtube model. The streamtube-based sectional model is able to provide an accurate solution of model equations within a reasonable computing time. For a number of studies, one-dimensional simulations are sufficient. Flow dependence can be taken from CFD simulations, flow correlations, or from experimentally-based estimates of time-temperature histories. While the focus is on the sectional method, a bivariate extension of the quadrature method of moments (QMOM) has also been tested. The method is shown to be able to provide reasonable computational representations of aerosol particle shape evolution. The models have been used to analyse various cases of aerosol formation, growth and deposition.

Aerosol formation and growth dynamics simulations are used in analyses of aerosol formation experiments in a laminar flow reactor, experiments of particle property evolution in a counterflow diffusion flame reactor, and aerosol formation mechanisms in recovery boilers. Computational simulations of recovery boilers demonstrate the feasibility of Na_2SO_4-route fume formation mechanism theory. The accordance between particle size distribution predictions and experimental data is fairly good.

Model studies of deposition provide insights into the transfer mechanisms of fly ash particles and inorganic vapours to the heat transfer surfaces of industrial boilers. Estimates of deposition velocities are obtained for particles of various sizes and inorganic vapours under various conditions. An area in which aerosol dynamics and transport processes are especially significant is the case of alkali chloride deposition. For these species, there seems to be a great deal of variation

in the proportions of particle and vapour deposition in the typical temperature range of biofuel fired boiler superheater conditions. In recovery boilers, particle deposition is predicted to be the dominant final alkali chloride deposition mechanism for freshly soot-blown superheater surfaces, while direct vapour deposition can be equally important when there is an insulating deposit layer, and, consequently, higher temperatures at the deposit surface. The total rate of alkali chloride deposition does not have as strong a temperature dependence. While homogeneous nucleation is predicted to be negligible in recovery boiler superheater tube boundary layers, the reverse is true for conditions resembling fluidised beds during bio- and mixed fuel combustion. The relationship between deposit-related problems, such as fouling, slagging and corrosion, and the rate of deposition is not necessarily straightforward. Initial steps have been taken to simulate deposit transformations in order to provide computational demonstrations of the implications of alkali chloride deposition. A model that links alkali chloride deposition to the presence of HCl in the deposit-metal interface has been developed and illustrative simulations have been carried out.

Overall, the models are shown to provide an insight into aerosol dynamics and transport phenomena in various systems. It is noted that the development of a universal CFD-based aerosol model is difficult. Instead, it is often more appropriate to make suitable simplifying assumptions, such as a parabolic flow, a constant size distribution shape or a reduction to one dimension. Suitable assumptions allow the use of computationally efficient and accurate methods. These make it possible to extend the scope of modelling beyond aerosol issues, for a more extensive analysis.

Academic dissertation

Helsinki University of Technology, Systems Analysis Laboratory

Supervising Professor:	Raimo P. Hämäläinen, Helsinki University of Technology
Supervisor:	Dr. Jorma K. Jokiniemi, VTT Processes, Espoo
Preliminary examiners:	Prof. Markku Kulmala, University of Helsinki
	Dr. Jaakko Saastamoinen, VTT Processes, Jyväskylä
Official opponent:	Dr. Athanasios G. Konstandopoulos, Centre for Research and Technology – Hellas, Chemical Process Engineering Research Institute, Thessaloniki, Greece

Preface

The research work for this thesis was carried out mainly in the Aerosol Technology Group of VTT Energy. I wish to express my gratitude to my supervisor, Dr. Jorma Jokiniemi, for his knowledgeable guidance and enthusiasm towards scientific work. I would like to thank all my colleagues in the group for an extraordinarily inspiring working atmosphere. I am indebted to Prof. Daniel Rosner for his expert supervision during my exchange research in the High Temperature Chemical Reaction Engineering Laboratory of the Department of Chemical Engineering at Yale University, New Haven, USA. I also wish to thank my labmates of that time for their pleasant company. In addition, I would like to acknowledge Prof. Raimo Hämäläinen and my pre-examiners, Dr. Jaakko Saastamoinen and Prof. Markku Kulmala, for their contributions.

I would like to express my gratitude towards all of my co-authors and other people that have been involved in the research. Especially, I would like to thank Dr. Pirita Mikkanen for her continuous encouragement and productive co-operation and Dr. Kari Lehtinen for his invaluable support and advice. In addition, I have greatly benefited from fruitful discussions with Dr. David Brown, Mr. Arkke Eskola, Dr. Tommy Jacobson, Prof. Esko Kauppinen, Dr. Terttaliisa Lind, Mr. Jussi Lyyränen, Dr. Robert McGraw, and Dr. Tuomas Valmari.

The funding for this work is gratefully acknowledged: the Finnish National Technology Agency (Tekes), the Academy of Finland, VTT Energy and the companies Fortum Power and Heat Oy, Andritz-Ahlstrom Oy, Kvaerner Pulping Oy, and Wartsila Diesel Oy. This overview of the author's research was written with the support of a grant from the Imatran Voima Foundation.

Finally, I want to thank all of my family and friends for their support over the years.

List of publications

A Jokiniemi, J., Pyykönen, J. Mikkanen, P. and Kauppinen, E. (1996) Modeling fume formation and deposition in kraft recovery boilers. *Tappi J.* 79, 171–181.

B Jokiniemi, J., Pyykönen, J., Lyyränen, J., Mikkanen, P. and Kauppinen, E. (1996) Modelling ash deposition during the combustion of low grade fuels. In: *Applications of Advanced Technology to Ash-Related Problems in Boilers.* Eds. Baxter, L. and DeSollar, R. (Plenum Press, New York), 591–615.

C Pyykönen, J., Jokiniemi, J. and Jacobson, T. (1999) Development of a prediction scheme for pulverised coal-fired boiler slagging. In: *Impact of Mineral Impurities in Solid Fuel Combustion.* Eds. Gupta, R. Wall, T. and. Baxter, L. (Kluwer Academic / Plenum Publishers, New York), 735–752.

D Pyykönen, J. and Jokiniemi, J. (2000) Computational fluid dynamics based sectional aerosol modelling schemes. *J. Aerosol Sci.* 31, 531–550.

E Pyykönen, J. and Jokiniemi, J. (2001) Model studies of deposition in turbulent boundary layer with inertial effects. Proceedings of the VIII Finnish National Aerosol Symposium. Report Series in Aerosol Science 54, Finnish Association for Aerosol Research. 28–38.

F Rosner, D. and Pyykönen, J. (2002) Bi-variate moment method simulation of coagulating and sintering alumina nano-particles in flames. Accepted for publication in *AIChE J*.

G Pyykönen, J. and Jokiniemi, J. (2002) Modelling alkali chloride superheater deposition and its implications. Submitted for publication in *Fuel Process. Technol.*

Author's contribution

This dissertation consists of an overview of the author's research and a selection of his publications. The work was carried out at the VTT Aerosol Technology Group of VTT Energy, Finland (publications A–E, G) under the supervision of Dr. Jorma Jokiniemi, and at the Chemical Engineering Department of Yale University, United States (publication F) under the supervision of Prof. Daniel Rosner. The publications are in chronological order.

Papers A and B deal with aerosol dynamics in recovery boilers. Paper A presents a theory of fume formation in recovery boilers, suggested by Dr. Jorma Jokiniemi, and computational simulations of aerosol dynamics, carried out by the author, that demonstrate the feasibility of the theory. In addition, Papers A and B discuss deposition mechanisms in recovery boilers. Paper B presents the deposition models and, in addition to dealing with recovery boilers, provides a rudimentary analysis of deposition mechanisms in medium-speed diesel engines. Paper C describes a computational fluid dynamics- (CFD) based slagging prediction scheme for pulverised coal combustion. The scheme was developed and implemented jointly with Dr. Tommy Jacobson of the IVO Technology Centre (currently Fortum Heat and Power Oy). Paper D presents two CFD-based sectional models of aerosol dynamics and transport. The development of these models was partly motivated by the fume formation studies presented in Paper A, and partly by nuclear safety-related issues. Papers E and G include an evaluation and development of selected key aspects of deposition models presented in Paper B and applied in Papers A–C. The studies made use of the CFD-based aerosol models presented in Paper D. Paper F presents an implementation of a bivariate quadrature method of moments (QMOM)- based aerosol model. The model is used for analysing particle size and shape evolution in a one-dimensional flame.

The author wrote Papers A and B on the basis of drafts for the sections describing the theory by Dr. Jorma Jokiniemi. Papers C–E and G were written by the author. Prof. Daniel Rosner wrote Paper F on the basis of a draft by the author for the sections that discuss the model's implementation and the results of the simulations.

Contents

Appendices of this publication are not included in the PDF version. Please order the printed version to get the complete publication (http://otatrip.hut.fi/vtt/jure/index.html)

List of symbols

a_p	particle surface area
a_{sph}	surface area of volume equivalent sphere
A	Stoichiometric conversion coefficient
$\boldsymbol{c}$	composition vector
C	empirical correction factor for nucleation rates
d_{coll}	collision diameter of particle
d_{gyr}	gyration diameter of particle
d_p	particle diameter
d_p^*	diameter of critical cluster
d_v	geometric volume mean diameter
d_1	spherule (primary particle) diameter
D_B	particle Brownian diffusivity
D_{eff}	effective vapour diffusivity in a porous medium
D_f	fractal dimension
D_v	diffusivity of vapour
e_p	excess surface area of a particle
e_i	excess surface area of a particle at quadrature point i
E_s	activation energy for sintering by surface diffusion
J_{Dep}	deposition flux
J_{Fr}	nucleation rate according classical theory (Frenkel, 1955)
J_{Gi}	nucleation rate according to Girshick and Chiu (1990)
k	Boltzmann constant
k_f	prefactor in fractal law
k_g	gas thermal conductivity
k_s	effective surface roughness
Kn_g	Knudsen number (for gas)
Kn_v	Knudsen number for vapour
L	latent heat of condensation
m	particle mass concentration
m_m	mass of a molecule
m_p	particle mass
M	total particle mass concentration
$M_{k,l}$	bivariate moment
M_v	molecular weight of condensable vapour

n	particle number concentration
N	total particle number concentration
N_m	mass transfer resistance term
N_{out}	total particle number concentration at reactor outlet
N_T	heat transfer resistance term
N_q	number of quadrature points
N_S	effective number of spherules in a particle
p_s	saturation vapour pressure
r	radial co-ordinate for superheater tube or flow reactor
R	universal gas constant
S	saturation ratio
S_r	saturation ratio at particle surface
S_∞	saturation ratio in the free stream
t	time
T	temperature
T_L	Lagrangian time scale of turbulence
$\boldsymbol{u_g}$	gas velocity
$\boldsymbol{u_p}$	convective particle velocity component due to turbophoresis-inertia
$\boldsymbol{u_{th}}$	thermophoretic particle velocity component
$\boldsymbol{u_{ti}}$	particle velocity component due to turbophoresis-inertia
u_*	friction velocity
v	vapour concentration
v_{eq}	equilibrium vapour concentration
v_i	particle volume at quadrature point *i*
v_m	molecular volume
v_p	particle volume
V_{dep}	deposition velocity
w_i	weight of quadrature point *i*
x	co-ordinate parallel to the surface
$\boldsymbol{x}$	position vector
X	dimensionless neck width (the ratio to particle diameter)
y	co-ordinate perpendicular to the surface
z	axial co-ordinate for laminar flow reactor or co-ordinate perpendicular to the stagnation plane in the counterflow diffusion flame reactor
z_{NaCl}	mass concentration of condensed NaCl
β	collision frequency function

β_M	transition regime correction for mass transfer resistance
β_T	transition regime correction for heat transfer resistance
δ	Tolman length
μ	viscosity
ρ_c	condensed phase density
ρ_g	gas density
ρ_p	particle density
σ	surface tension
σ_∞	macroscopic surface tension
τ_f	characteristic fusion time

Subscripts

∞	free stream
y	component perpendicular to the wall

Superscripts

+	dimensionless with respect to characteristic boundary layer time and length scales (see paper E)
‘	turbulent fluctuation component

1. Introduction

Suspensions of small solid or liquid particles in gases, called aerosols, are important in many fields, such as combustion processes, flue gas cleaning technology, nuclear safety, materials processing, the pharmaceutical industry, and atmospheric sciences. The smallest aerosol particles are in the size range of molecules, while one hundred micrometres is usually regarded as the upper limit of the definition. Often, aerosol particle populations are not stable but undergo constant evolution as a consequence of new particle formation via homogeneous nucleation and disintegration, condensation and surface reactions on the particles, collisions amongst the particles that result in agglomeration, and various physical and chemical phenomena that occur within the particles. Aerosol particles can also be transported along a gas flow and experience changes in the surrounding physico-chemical conditions, possibly under the influence of turbulence. Particle transport can also be affected by inertia, gravitation, and particle diffusion, as well as thermophoresis and other phoretic effects.

This thesis deals with aerosol dynamics and transport modelling. There can be many motivations for modelling. In some cases, little is known about the system. For such systems, a representation in the form of a computational model can give an insight into the importance of various factors and provide a platform for testing various hypotheses. For better-known systems, a model can provide quantitative predictions of its behaviour in different conditions, and thus, guide its operation and design.

The main objective of thesis work has been to develop models that improve understanding of aerosol formation and deposition mechanisms in various industrial systems, in particular in combustion processes. The models are supposed to assist in identifying the importance of different factors in various industrial aerosol issues and provide a link between lab-scale experiments and industrial processes. Since industrial aerosol systems are frequently chemically complex, and the details of their behaviour are poorly understood, the goals of modelling are mostly in the realm of acquiring insight into systems of which little is known. Much of the work has been motivated by general needs of industrial process-oriented aerosol behaviour analysis. An issue of which better

understanding has especially been desired is deposition on heat exchanger surfaces in combustion processes.

Complex flow fields and aggregate particle structures, which are typical features in industrial systems, have required the development of new modelling methods. Extension of the sectional model to multiple spatial dimensions and the creation of a moment-based model of the structural evolution of aggregate particles have been specific targets of this research. An important requirement for modelling tools is that they should be reasonably efficient and not distorted by spurious numerical effects. Models of aerosol transport and dynamics can involve many state variables, complex submodels, and multiple spatial dimensions. Therefore, the selection of appropriate models for various investigations requires careful consideration and an insight into their properties, such as computational efficiency and accuracy.

The crux of the thesis, the computational methods, is presented in Chapter 2. The general dynamic equation is introduced and various ways of representing distributions of aerosol properties are discussed. Model development has provided tools for the simulation of aerosol behaviour in real multidimensional situations and in cases where more than one characteristic of aerosol particles is significant. New model development has been carried out in coupling aerosol simulations with computational fluid dynamics (CFD), improving the efficiency of the sectional method, and testing the suitability of the quadrature method of the moments model for real-world bivariate cases, in which not only particle size but also particle shape is a consideration. The application of the presented computational methods for the analysis of various systems is discussed in subsequent chapters.

Chapter 3 discusses the application of the models for studies of aerosol formation and aerosol property evolution. Aerosol formation dynamics depends on the interplay of the kinetics of homogeneous nucleation and heterogeneous condensation. In many cases, collisions of particles that result in agglomeration may also play a role. Particle growth is governed by heterogeneous condensation and agglomeration. For condensation, gas-phase chemistry is an important consideration. Another important factor is the evolution of particle structure under simultaneous agglomeration and particle sintering.

Chapter 4 discusses the application of the models for deposition studies. In many combustion processes, the formation of ash deposit layers is a cause of significant fouling, slagging and corrosion problems (e.g. Bryers, 1996; Couch, 1994). The models of aerosol behaviour allow a detailed study of the mechanisms of fly ash particle and vapour-phase fume transport to deposit layers. Two phenomena are subjected to closer investigation. These are particle and vapour co-deposition, when boundary layer aerosol dynamics is important, and particle deposition under the influence of inertia in turbulent boundary layer eddies. In addition, the implications of deposition mechanisms for the evolution of ash deposit properties are discussed.

Chapter 5 summarises the implications of the modelling studies for various real-world systems. These include fume formation and deposit formation in recovery boilers, as well as deposition mechanisms in fluidised beds during bio- and mixed fuel combustion and in heavy-duty diesel engines during low-grade heavy fuel oil combustion. In addition, a slagging prediction scheme for pulverised coal combustion is presented. Part of the motivation for studies of aerosol formation arose from nuclear reactor accident scenarios that involve revaporisation. This background is briefly reviewed, though early experiments led to the abandonment of large modelling efforts in this field.

2. Modelling methods

2.1 The general dynamic equation

Aerosol particle transport and dynamics can be represented mathematically by a population balance equation, usually referred to as the general dynamic equation (e.g. Friedlander, 2000). It can be represented in a number of different ways, depending on the scope of the phenomena included. If multiple spatial dimensions are included, it is a convective-diffusive equation with source terms for aerosol dynamics. For the purposes of this work, the general dynamic equation is given in terms of differential turbulence-averaged (overbar) particle mass concentration density function $\overline{m} = \overline{m}(\mathbf{x}, v_p, a_p, \mathbf{c}, t)$, where $\boldsymbol{x}$ denotes position, v_p particle volume, a_p particle area, $\boldsymbol{c}$ composition, and t time:

$$\frac{\partial \overline{m}}{\partial t} + \nabla \cdot \left(\overline{\left(\mathbf{u}_g + \mathbf{u}_{th} + \mathbf{u}_{ti}\right) m} - D_B \rho_g \nabla \overline{\left(\frac{m}{\rho_g} \right)} \right) = \overline{\left(\frac{\partial m}{\partial t} \right)}_{Nucl} + \overline{\left(\frac{\partial m}{\partial t} \right)}_{Cond} + \overline{\left(\frac{\partial m}{\partial t} \right)}_{Agg} + \overline{\left(\frac{\partial m}{\partial t} \right)}_{Sint} . \quad (1)$$

Here $\boldsymbol{u_g}$ is the gas velocity, $\boldsymbol{u_{th}}$ and $\boldsymbol{u_{ti}}$ are the particle drift velocities due to thermophoresis and turbophoresis inertia, respectively, ρ_g is the gas density, and D_B is the Brownian diffusivity of the particle. The left-hand side of the equation has terms that refer to temporal, convective and diffusive rates of change in the differential particle mass concentration. The right-hand side has source terms for aerosol dynamics due to nucleation, heterogeneous condensation, agglomeration, and sintering.

The adopted form of the general dynamic equation indicates that a number of different aspects, such as spatial and temporal variation, particle size, shape, and chemical composition distributions, need to be considered. This multitude of dimensions presents a formidable computational challenge for the creation of a general accurate model. For practical simulations, it is better to assess what kind of simplifications can be made and include in the model only the aspects that are essential to the problem at hand. A number of phenomena that are not considered in this research have been omitted from the general dynamic equation

here. These include such phenomena as gravitation, electrostatic forces, surface chemistry, intra-particle transport, and the effects of turbulent micro-mixing. Turbulence has only been considered in the case of boundary layers. The turbulence-averaged formulation is included here for the sake of completeness. In the simulations, the treatment of turbulence is an approximation based on Guha (1997) and is discussed in Section 4.2.

For a complete representation, the general dynamic equation for aerosol particles is complemented with dynamic equations for turbulence-averaged condensable vapour mass concentration density functions $\overline{\mathrm{v}}_j = \overline{\mathrm{v}}_j(\mathbf{x},t)$, where j is the species number index, given by:

$$\frac{\partial \overline{\mathrm{v}}_j}{\partial t} + \nabla \cdot \left(\overline{\mathbf{u}_g \mathrm{v}_j} - D_{v\,j} \overline{\rho_g \nabla \left(\frac{\mathrm{v}_j}{\rho_g} \right)} \right) = - \overline{\left(\frac{\partial m\left(d_p^*\right)_j}{\partial t} \right)}_{Nucl} - \overline{\left(\frac{\partial M_j}{\partial t} \right)}_{Cond}, \tag{2}$$

where m(d_p*) is the mass concentration of the critical nuclei (of diameter d_p*), $M_j = M_j(\mathbf{x},t)$ is the total particle mass concentration of species j, and $D_{v\,j}$ is the vapour diffusion coefficient. Vapour is depleted by gas-to-particle conversion via nucleation and heterogeneous condensation.

2.2 Representation of particle property distribution

A number of different ways can be used for representing the size, shape, and chemical composition distributions of aerosol particles when the evolution of these distributions is modelled (e.g. Ramkrishna, 2000). Here the discussion is restricted to temporal evolution in the absence of transport phenomena. Conceptually, the simplest way is to observe the behaviour of a large number of computational particles. This is called the Monte-Carlo method. The method allows for a straightforward simulation of problems in which particles need to be described by a large number of internal state variables. Arbitrarily complex interactions between various state variables can be handled easily. The

disadvantage of the Monte-Carlo method is the large number of computational particles required for accurate simulations and the resulting demands on computer time. Nevertheless, the method has been successfully used for studying certain aspects of aerosol dynamics, such as the evolution of particle shape characteristics (e.g. Tandon and Rosner, 1999; Rosner and Yu, 2001).

Another method, the sectional method (Papers A–D), is based on discretising the particle property domain along each state variable (see reviews by Seigneur *et al.*, 1986; Jacobson and Turco, 1995). The equations of the evolution of particle concentration in each discretised property domain section are solved. No assumptions regarding the shape of the distribution need to be made. In multivariate problems, the computational requirements can become very large (Xiong and Pratsinis, 1993). These requirements can be alleviated with appropriate simplifying assumptions. For instance, it can be assumed that all particles within one size section are of similar chemical composition (Papers A, B, D, and G). This approach is able to provide average chemical compositions, which is sufficient for a large number of simulations. Homogeneous nucleation and condensation growth without significant coagulation provides an example of a process where particles of the same size are expected to be similar. If significant coagulation is involved, there can be particles of various chemical compositions in one size section and only averages are obtained. A full representation of the size-dependent chemical composition distribution is required if there are phenomena that are strongly dependent both on particle size and chemical composition. This is the case, for instance, if one chemical component is subject to evaporation during coagulation that is mild enough not to average compositions.

Moment methods make it possible to describe particle property distribution with a limited number of moments that represent integral properties of the distributions (see review by Whitby and McMurry, 1997). The moments can be multivariate. In the simulations of aerosol dynamics, the evolution of the moments is tracked. This implies that the actual shapes of the distributions are not directly considered, and the methods are, in that sense, approximate. The advantage is that the methods are computationally very efficient and often, for practical purposes, the moments carry sufficient information about the aerosol. To calculate the source terms for the evolution of moments, information about particle size distribution is required and, consequently, some assumptions are

required. In the most common type of moment methods, a shape is assumed for the distribution. The lognormal and multi-modal lognormal shapes are practically relevant common assumptions for representing particle size distribution. A model comparison between the lognormal and the sectional model in a one-dimensional nucleation-condensation case demonstrated that, while the lognormal model can predict the overall features of aerosol formation surprisingly well, there are still significant differences in the predictions of resulting particle number concentrations (Brown *et al.*, 1998).

In the quadrature method of moments (QMOM), a surrogate size distribution that consists of a number of quadrature points is constructed, based on the moments (McGraw, 1997; Wright *et al.*, 2001, Paper F). The size distribution is assumed to be represented by a set of the quadrature points that yields the moments of the distribution. A quadrature point, *i*, is characterised by a set of property values and a weight, w_i. Initial steps in bivariate simulations of real-world processes have been taken for a simulation of a sintering aerosol with particle volume v_p and excess area $e_p = a_p - a_{sph}$ as the state variables (paper F), where a_p is the area of the particle and a_{sph} is the area of a sphere of equivalent volume. Bivariate moments $M_{k,l}$ are defined as:

$$M_{k,l} = \int_0^\infty \int_0^\infty v_p^k e_p^l n(v_p, e_p) dv_p \, de_p \tag{3}$$

An N_q-point quadrature expression with quadrature points $\{v_i, e_i, w_i\}$ is

$$M_{k,l} \approx \sum_{i=1}^{N_q} v_i^k e_i^l w_i \tag{4}$$

The key in the QMOM is the mathematical method that allows the optimal estimation of the quadrature points when the moments are known. This makes it possible to repeatedly switch between evolving the moments and calculating the evolution rates based on the momentary quadrature points. The study by Wright *et al.* (2001), in idealised constant continuum regime conditions with volume and area as state variables, showed that the method can provide accurate estimates of agglomeration-sintering phenomena. However, the case they considered was not truly bivariate since, with constant fractal dimension, no

terms in the determination of the moment evolution rates were dependent both on particle volume and area. This made it possible to solve volume and area distributions independently with different sets of weights. In Paper E, a realistic case that necessitates a true bivariate (volume and excess area) simulation was carried out (see section 3.5). The agglomeration coefficient was defined as a function of both particle volume and area. In addition, the study involved free molecular regime, and consequently, more variation in the agglomeration kernel than in the continuum regime. The results indicated that the bivariate QMOM is suitable at least for rough estimates. Only a three-point (N_q=3) quadrature was successfully employed in this study. Further development, to increase the number of quadrature points, is required to improve the accuracy of the method. An advantage of the QMOM is that it can easily be implemented in the same code as the sectional method and the methods can share aerosol dynamics submodels. One vision for the bivariate QMOM is that it could be used to set up a case with rough initial estimates, while the sectional model can provide the accurate result. The univariate QMOM is sufficiently accurate for the requirements of many practical simulations in its present form.

In addition to the distribution shape assumption and the quadrature method, a third possible way of using the moment method is to generate a set of smooth model distributions that have the specified moments and then average these (Wright, 2000).

2.3 Simulation methods for multiple spatial dimensions

In many practically relevant cases, aerosol transport and dynamics takes place in flow systems with spatial variation. For such cases, a one-dimensional simulation along the main flow path is frequently sufficient to capture the relevant aerosol phenomena. This is the case, for instance, if one studies the chemistry aspects and the time scales of aerosol formation and growth mechanisms in industrial boilers (Papers A and B). Computational requirements of a full 3D aerosol simulation embedded in computational fluid dynamics (CFD) are much larger than those of a 1D simulation. Indeed, if the primary interest is in the study of the fundamental aspects of aerosol behaviour, the experiments should be designed in such a way that 1D simulations are possible. A good example is the counterflow diffusion flame reactor, where the dynamics

essentially takes place in one direction (Xing *et al*., 1996; Xing, 1997). A CFD simulation can provide the time-temperature history of a fluid parcel that moves along the stagnation line, and the data can be used as input for aerosol dynamics simulations (Paper F). The commercial CFD code Fluent (Fluent, 1996) was used in all CFD simulations covered here. As aerosol phenomena often involve time scale variations of many orders of magnitude, adjustable time/space steps are essential for computational efficiency in 1D simulations. If there is significant streamwise diffusion (laminar or turbulent) involved, a single pass space-marching solution is not sufficient. Instead, transport equations with diffusion terms must be solved (Paper G). Implicit methods that use a tridiagonal matrix algorithm provide an efficient solution strategy. For some flow fields, such as boundary layer flows, correlations can be used instead of CFD simulations to provide the flow and temperature fields (Papers E and G).

Numerous aerosol systems are such that the flow is of a parabolic nature. This means that boundary layer approximation of neglecting streamwise diffusion (laminar or turbulent) is valid and efficient boundary layer solution methodologies can be used. Paper D presents a boundary layer-type solution method, termed the streamtube method, embedded in a CFD code for aerosol studies on top of a CFD solution. In contrast to standard boundary layer codes, transport in the direction perpendicular to the flow (or surface) is not calculated at every aerosol dynamics simulation step, but cross-streamtube cells are created out of a number of these steps (Fig. 1). This is done to enhance computational efficiency. The streamtube methodology allows for adjustable streamwise space steps and, consequently, makes it easy to deal with the sharp streamwise gradients and large time scale variations often encountered in nucleation cases. The aerosol dynamics simulation grid is independent of the CFD simulation grid, which eliminates any additional computational burden on CFD flow simulations. For boundary layer problems, the incorporation in CFD makes possible the rigorous analysis of non-isothermal flows and allows a finer grid for aerosol transport studies than is necessary for the flow simulation (Paper E). Whenever the streamtube methodology is applicable, the sectional method can be used with good computational efficiency and accuracy, as demonstrated in Paper D. The scheme has been developed for systems where the effect of aerosol dynamics on the flow is negligible. The effect of condensation heat release on aerosol dynamics can, however, be considered in an approximate way. A more

extensive coupling is, at least in theory, possible via iteration between the aerosol and CFD simulations.

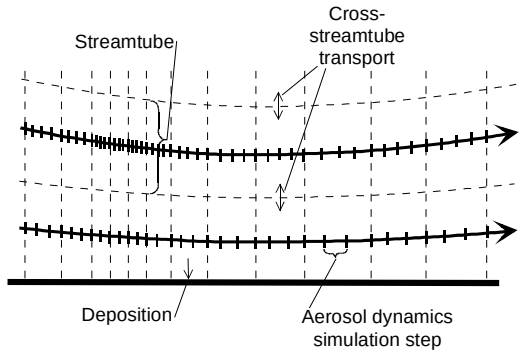

Figure 1. Schematic representation of the streamtube scheme (paper D).

Full Eulerian simulations with standard CFD routines for arbitrary scalar variables are general for any elliptic flow. Two-way coupling is easily implemented. However, the computational requirements are large if the sectional approach is used. Problems that include nucleation are especially hard to solve, since the cases can encompass a large variation in time scales. Short nucleation time scales necessitate very fine grids in the region where nucleation takes place. Papers D and G explore the limits of the sectional approach for full Eulerian CFD simulations. If the location of the nucleation zone is not known beforehand, as in the non-isothermal laminar flow reactor (Paper D), the computational requirements proved to be too large for accurate results, at least in the case that no automatic grid adjustment capabilities are available. On the other hand, if the location of the nucleation zone is known approximately in advance, as in boundary layer nucleation (Paper G), acceptably accurate results can be obtained. When dealing with full Eulerian simulations, one should carefully consider if a sectional scheme is really required. Often the simulations of complex elliptic flows are accompanied by a number of uncertainties, which makes the better accuracy of the sectional method, as opposed to, say, moment methods, a subtlety. Moreover, for cases that involve condensation, a large number of bins is required to combat numerical diffusion in the particle size space, in order to achieve accuracy superior to that of CFD-based moment methods, such as those of Brown (1996), Whitby and Hoshino (1996), and Wilck and Stratmann (1997). For some real-world cases, the details of the

chemical phenomena in aerosol formation are poorly known and it is more appropriate to use correlation-based overall kinetic models, rather than a proper aerosol model. This is the case, for instance, when modelling soot formation and burnout as part of large boiler simulations. Recently, there has been some research in the challenging area of CFD-based aerosol simulations during turbulent mixing (Wu and Menon, 2000; Garrick *et al*., 2001).

2.4 Techniques for the sectional approach

With today's computational facilities, simulations of aerosol dynamics with particle size and size-related average chemical composition as the state variables present no computational problems. Computational considerations become important when moving on to multiple spatial dimensions or to more state variables. Both stationary grid methods, where the particle sizes associated with different bins remain fixed (e.g. Sutugin and Fuchs, 1970; Gelbard *et al.*, 1980; Raes and Janssens, 1986; Jokiniemi *et al.*, 1994), and moving grid methods, where condensational growth is represented by moving the bins along the particle size axis (e.g. Mordy, 1959; Gelbard, 1990), have been presented in the literature. Both nucleation and coagulation have been included in moving grid-based schemes (Murata *et al*., 1989; Simonsen and Livbjerg, 1992; Young, 1992; Sher and Jokiniemi, 1993; Christensen, 1995; Kumar and Ramkrishna, 1997). Paper D presents a computationally efficient version of the univariate sectional model for the purposes of streamtube calculations. The premise for the development of the model was the observation that it is the large number of bin pairs that need to be considered for agglomeration that creates the heaviest computational burden. A large number of bins is required to combat numerical diffusion in the particle size space during heterogeneous condensation. A moving grid is computationally efficient and eliminates all significant numerical discretisation errors for nucleation-condensation processes. The effects of numerical diffusion associated with the stationary grid are clearly visible in the predictions of particle size distributions in the left-hand graph of Fig. 2. These are from the simulations of Wagner's (1982) experiments of particle growth via water condensation on initially monodisperse 0.02 μm particles. The reason for using a stationary grid is that it is required for the efficient modelling of cross-streamtube transport. To retain the advantages of both of the grid schemes, a coupled stationary and moving grid system was developed. Transport is

computed with the stationary grid, while nucleation and condensation are calculated with the moving grid. It is better to use the stationary grid for agglomeration. This enables a relatively sparse bin density for the computationally demanding calculations of transport and agglomeration, while the demands on bin density to achieve accuracy are modest. The right-hand graph in Fig. 2 demonstrates that even a modest bin density is sufficient in the simulation of an agglomeration process, in this case that of TiO_2 particles starting from stable molecules. A dense grid can be used for nucleation and condensation processes, without a great computational burden.

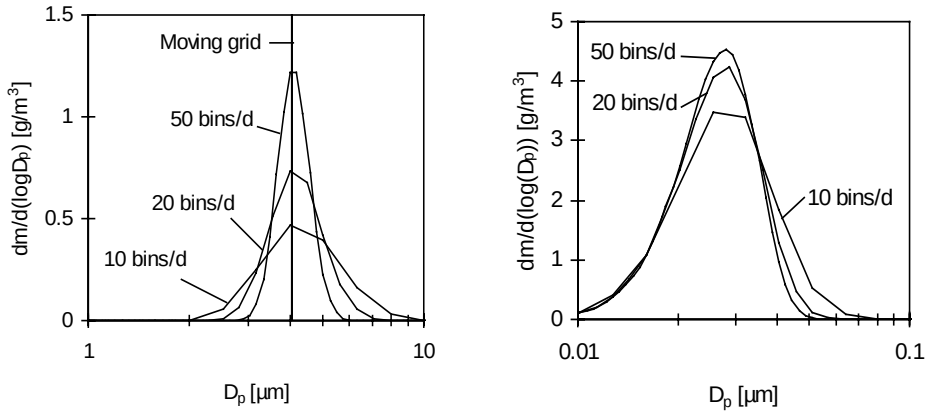

Figure 2. Studies of the numerical accuracy of the sectional scheme with various bin densities. Simulated particle size distributions in heterogeneous condensation (left) and coagulation (right) (Paper D).

The primary grid in the coupled grid simulations is the moving grid. Nucleation is modelled by inserting new bins of the size of the critical embryo into the grid. Care is taken to merge two successive bins if the ratio of the particle diameters they represent goes below a certain predefined value during condensation growth. For the calculation of coagulation, the stationary grid particle size distribution is first generated out of the moving grid distribution, using a mass and number-conserving size split technique (e.g. Raes and Janssens, 1986). The agglomeration and transport rates are then estimated, based on the stationary grid concentrations. Finally, these are given as source terms to the moving grid bin concentrations. They are partitioned, using the size-split technique in reverse. Information concerning the fractional moving grid bin concentrations attributed to each stationary grid bin is stored. Partitioning from the stationary

grid back to the moving grid is done in proportion to these fractional concentrations. In the case that there is no moving grid bin attributed to a stationary grid bin that has a non-zero agglomeration or transport source term, a new moving grid bin is created. For cases when condensation processes are of secondary importance, the scheme has a completely stationary grid-based option. Additionally, this scheme includes the possibility of a fine grid for nucleation and condensation and a sparse grid for coagulation and transport.

3. Topics in aerosol formation and growth

3.1 Nucleation as the basis of particle size distribution

Homogeneous nucleation is an important phenomenon in the formation of particle size distribution. Molecular collisions result in molecular clusters. These are always present even in an unsaturated gas. Small molecular clusters are not stable, since surface forces are not strong enough to keep the molecules attached. If the vapour is supersaturated, there can be large molecular clusters for which, as a result of further molecular collisions, the rate of growth is larger than that of disassociation. The cluster size at which the evaporation of molecules and growth by the addition of molecules have equal probabilities is called the critical size. The higher the saturation ratio *S*, the higher the concentrations of molecular clusters and the smaller the critical cluster size. Using the Kelvin relation, it can be shown that the critical cluster diameter d_p^* is given by (e.g. Friedlander, 2000):

$$d_p^* = \frac{4\sigma v_m}{kT \ln S}, \tag{5}$$

where σ is the surface tension of the condensable species, v_m its molecular volume, *k* the Boltzmann constant, and *T* the temperature. The starting point for models of nucleation rates is the classical nucleation model (Frenkel, 1955), which provides the nucleation rate J_{Fr} as particles in unit time and unit volume

$$J_{Fr} = \frac{\mathrm{v}^2}{\rho m_m}\sqrt{\frac{2\sigma}{\pi m_m}}\exp\left(-\frac{\pi\sigma d_p^{*2}}{3kT}\right), \tag{6}$$

where m_m is the mass of a molecule of the condensable species. There are many variants of the classical nucleation theory. In Paper C, a modification that enforces the Gibbs free energy of monomers to zero is applied. This self-consistent correction nucleation model, by Girshick ans Chiu. (1990), gives the nucleation rate J_{Gi} as:

$$J_{Gi} = \frac{1}{S} \cdot \exp\left(\frac{\sqrt[3]{36\pi v_m^2 \sigma}}{k_B T} \right) \cdot J_{Fr} \tag{7}$$

An estimate of the particle surface tension as a function of particle size is provided by the Tolman equation, which is of a semi-empirical nature:

$$\sigma = \sigma_\infty \left(1 + 4\frac{\delta}{d_p} \right)^{-1}, \tag{8}$$

where σ_∞ is the macroscopic surface tension and δ is the Tolman length. Nucleation rates are extremely sensitive to surface tension values. The use of the Tolman equation in nucleation models is still a topic under discussion.

Due to deficiencies in mechanistic nucleation theories and the imperfect knowledge of physico-chemical parameters, especially at molecular dimensions, nucleation models need to be supplemented with empirical correction factors in order to allow realistic simulations. Paper C deals with a way of obtaining a correction factor for the nucleation rate from laminar flow reactor experiments. As these involve varying flow fields and simultaneous nucleation, heterogeneous condensation and diffusive vapour losses to the wall, an aerosol model embedded in CFD is required for rigorous estimates of nucleation kinetics. Paper C and a related study by Wilck and Stratmann were only concerned with obtaining a correction factor that multiplies the nucleation rate. Jensen *et al.* (2000) applied a method that involves two correction factors for the determination of alkali chloride nucleation kinetics. The empirical correction factors were included in the diffusion coefficient of the condensable vapour and the Tolman length, since these quantities were judged to be the most poorly-known key quantities. They were obtained from laminar flow reactor simulations that assumed a fully developed laminar flow profile.

In many engineering applications, the overall kinetics of aerosol formation when nucleation acts alongside heterogeneous condensation and coagulation is more important than nucleation kinetics as such. The interaction of these phenomena determines the resulting particle size distribution. A typical feature of aerosol dynamics in high temperature processes, such as the behaviour of inorganics in

combustion processes, is that there are rapid shifts in the saturation ratios, and therefore the time scale related to particle formation is short. When nucleation kinetics is very fast, the actual nucleation kinetics is not necessarily important, since a numerically large concentration of particles is formed in the nucleation zone. These particles coagulate very rapidly and the particle number concentration is, to a great degree, determined by the kinetics of coagulation. Fast nucleation very efficiently consumes condensable vapour and thus reduces the saturation ratio and suppresses further nucleation. This results in narrow nucleation zones, where most of the nucleation takes place. Further gas-to-particle conversion takes place by heterogeneous condensation. Continuous condensation on existing particles retains saturation ratios below the nucleation limit, which is much higher than that of heterogeneous condensation.

In the case that the rate at which supersaturating rises is not rapid and nucleation rates are not extremely high, it is possible that particle number concentration remains such that coagulation does not become significant. This was the case, for instance, in the laminar flow reactor experiments of DBP (dibutylphtalate) nucleation performed by Nguyen *et al*. (1987). In this case, it is the amount of particles that nucleate before significant nucleation is suppressed that determines the resulting particle number concentration. In laminar flow reactors, vapour diffusion and losses to the wall are also significant considerations. For a high molecular weight substance with more efficient heat transfer by conduction than mass transfer by diffusion, a nucleation front is formed in the middle of the reactor. Figure 3 shows a streamtube-based CFD model prediction of the number concentration that results from DBP nucleation as a function of saturator temperature. The temperature of the saturator determines the amount of condensable vapour. The predictions of Wilck and Stratmann (1997) are presented for comparison. Wilck *et al.* (1998) discuss the difficulty of validating nucleation theories as a result of the sensitivity of the simulations to imperfectly known physical data.

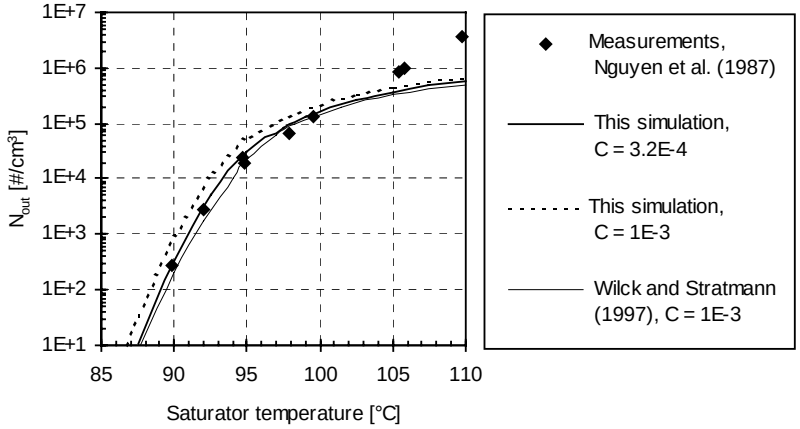

Figure 3. Mass flow averaged predictions with various correction factors C and measured values of outflowing particle number concentrations (N_{out}) as a function of the saturator temperature in the homogeneous nucleation experiments with DBP (Paper D).

An issue of practical relevance for model studies is often whether significant nucleation can occur in the presence of a small concentration of existing particles (seeds). This depends on the ability of the existing particles to scavenge vapour at a rate that can keep the saturation rates below the nucleation threshold. Figure 4 shows that, for DBP in the laminar flow reactor, nucleation is predicted to be suppressed at seed number concentration $1 \cdot 10^4$ #/cm^3, while the experimentally determined threshold concentration is larger. An additional consideration is that the dynamics of heterogeneous nucleation ("initial wetting") can delay the onset of heterogeneous condensation. This may lead to slightly higher saturation ratios and thus slightly favour nucleation.

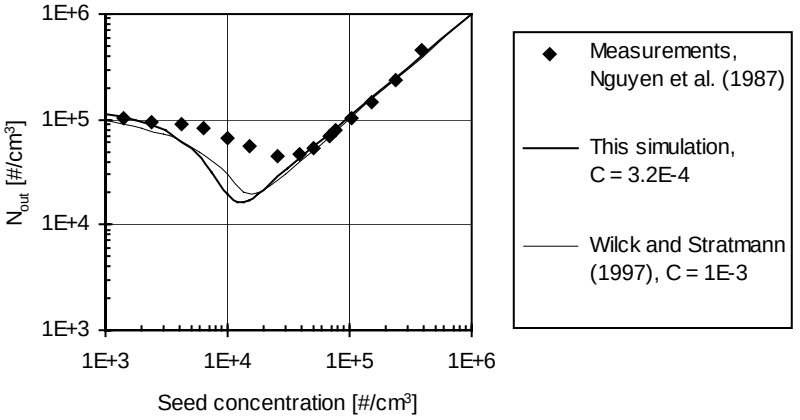

Figure 4. Mass flow averaged predictions and measured values of outflowing particle number concentrations (N_{out}) as a function of seed particle concentration in the heterogeneous nucleation experiments with DBP (Paper D).

3.2 Chemical reactions in condensation processes

In combustion processes, a chemical reaction is often involved in the nucleation process. If the reaction products of a chemical reaction have very low vapour pressures, they are in a highly supersaturated state and vigorous nucleation ensues. In many processes, such as pulverised coal combustion, the initial formation of fine mode fly ash particles takes place in the boundary layer of a burning fuel particle. Metal impurities are vaporised from the burning particle in a reduced form in the reducing conditions of the particle boundary layer. When the released molecules reach less reducing conditions away from the particle, metal oxides are formed. These have very low vapour pressures, and therefore they immediately nucleate to form a numerically large concentration of very small particles. These grow by agglomeration and later on they act as seed particles for the condensation of other species, such as alkali compounds.

Paper A discusses the reactions of alkali species with sulphur oxides, which result in the formation of alkali sulphate vapour, which has a low vapour pressure. As alkali hydroxides and chlorides are the most stable chemical species at high temperatures, the following reactions were considered:

$$2NaOH(g) + SO_2(g) + 1/2O_2(g) \rightarrow Na_2SO_4(g,c) + H_2O(g) \quad (9)$$

$$2NaCl(g) + SO_2(g) + 1/2O_2(g) + H_2O(g) \rightarrow Na_2SO_4(g,c) + 2HCl(g) \quad (10)$$

Here the reactions are given for sodium species and SO_2, but equivalent reactions with potassium and SO_3 are also possible, and at least for NaCl, more probable. The above reactions must be considered as overall bulk reactions. Anderson and Debnath (1983) have presented detailed reaction paths for the NaCl-to-Na_2SO_4 transformation that involve SO_3. Iisa *et al.* (1999) provide experimental evidence in the temperature range 900–1100°C that suggests that the reaction is, indeed, much faster with SO_3 than with SO_2. Christensen *et al.* (1998) suggested that the overall kinetics of KCl(g) to K_2SO_4(g) transformation could be approximated in such a way that the conversion is not limited by chemical kinetics in the time scales of industrial boilers above 812°C and no further reactions take place below this temperature. For NaOH sulphation, Steinberg and Schofield (1990) have presented detailed reaction paths that do not require SO_3 and can be relevant at high temperatures, where the availability of SO_3 may limit SO_3-based reactions. However, the bulk reaction rate by these pathways was estimated to be low for typical combustion conditions. The experimental data of Mikkanen *et al.* (1999b) suggest that the rate of alkali hydroxide sulphation can be sufficiently fast to be important for particle formation.

Whether alkali sulphate species vapour pressure rises sufficiently high for significant homogeneous nucleation to occur depends on nucleation kinetics and mixing processes. An additional consideration is that Na_2SO_4 may form as a result of a surface reaction on aerosol particles. In any case, the concentration of gas-phase Na_2SO_4 is predicted to be small, even if it may play an important role as a transient species. A chemical kinetics model, if available, or a gas-phase local equilibrium assumption in a cooling flow can be used to model the contribution of gas-phase reactions to the evolution of the gas phase composition. The model studies presented in Paper A have been confined to the local gas-phase chemical equilibrium assumption. The conversion of the reaction product (Na_2SO_4(g)) to a condensed form is considered to be limited only by the dynamics of gas-to-particle mass transfer.

3.3 Kinetics of the growth of particle size distribution

The mechanisms that account for particle growth are agglomeration and heterogeneous condensation. Heterogeneous condensation is understood here broadly to encompass, besides ordinary condensation, various surface reactions and adsorption processes that lead to material transfer from the gas phase to the particles. Agglomeration, when followed by instantaneous coalescence, is called coagulation, though there is some variation in terminology.

The effect of agglomeration on the evolution of particle size distribution is described by the following equation, where β is the collision frequency function (e.g. Friedlander, 2000):

$$\left(\frac{\partial n(v_p)}{\partial t}\right)_{agg} = \frac{1}{2}\int_0^{v_p} \beta(u_p, v_p - u_p)\, n(u_p)\, n(v_p - u_p)\, du_p - \int_0^{\infty} \beta(u_p, v_p)\, n(u_p)\, n(v_p)\, du_p \tag{11}$$

The first term is the rate of generation of particles of volume v_p due to collisions between smaller particles, and the second term is their rate of loss due to collisions with other particles. The dominant mechanism in industrial processes is Brownian agglomeration, which results from the Brownian motion of the particles. Fuchs (1964) has given a lengthy formulation of the Brownian collision frequency function that covers the whole particle size range from the free-molecular to the continuum regime. For the coagulation of particles of equal size, the Brownian collision frequency function is fairly constant throughout the whole size distribution spectrum. Coagulation-aged fine-mode aerosol particle size distributions are approximately lognormal, with geometric standard deviations less than 1.5, and condensation or particle growth from the free molecule regime to the continuum regime do not cause large changes in this shape. This implies that the direct dependence of Brownian coagulation rates on geometric mean particle size is not very strong. Naturally, there is the dominant indirect dependence that, under constant mass concentration, particle number concentrations are higher at smaller particle sizes, and, consequently, overall coagulation rates are higher as well. The effect of particle shape will be

discussed in Chapter 3.5. In isobaric processes, overall agglomeration rates decrease as a function of increasing temperature, since the effect of temperature-related increase in agglomeration coefficient is less important than that of concentration reduction as a result of the thermal expansion of the gas. It is the dependence of agglomeration rates on the square of the particle number concentration that makes this dependence dominant.

Many industrial processes are characterised by rapid nucleation that results in a high concentration of very small particles. The characteristic times of particle growth by Brownian agglomeration are very fast when particle number concentration is high. In the time scales of industrial boilers, agglomeration brings the particle number concentrations fairly rapidly to levels below $1 \cdot 10^9$ #/cm^3. Therefore, agglomeration is usually the dominant mechanism for initial growth or, at least, particles grow very rapidly by agglomeration if other mechanisms are not active as well. In the simulations of combustion processes, there is some uncertainty concerning electrical effects that, it has been noted, retard agglomeration of soot particles in some conditions (Haynes *et al.*, 1981). Later on, at larger particle sizes, turbulent kinematic agglomeration is a possibility. Still, for instance in boiler conditions, the kinematic agglomeration coefficients are considerably lower than the Brownian ones for the particle size ranges that are significantly affected by agglomeration. An open question is the magnitude of thermophoretic effects on agglomeration rates. These effects result from radiative heat transfer on particles. According to the theoretical studies of Mackowski *et al.* (1994), these may have some importance in the supermicron size range. At any rate, simulations with simple Brownian agglomeration kernels provide particle size distributions that are in a fair agreement with boiler measurements in superheaters and in the electrostatic precipitator (Paper A).

While initial formation and agglomeration determine particle number concentrations, their mass concentrations are determined by heterogeneous condensation. The rate of heterogeneous condensation can be modelled with the Mason equation, which considers both mass and heat transfer limitations on condensation rates (Mason, 1957). Heat transfer limitations are not significant for the condensation of trace amounts of vapour. The rate of change of particle mass m_p is given by

$$\frac{dm_p}{dt} = \frac{2\pi d_p \left(S_\infty - S_r\right)}{N_M / \beta_M + N_T / \beta_T}, \tag{12}$$

where

$$N_M = \frac{RT_\infty}{D_{v\infty} M_v p_s\left(T_\infty\right)}\ ,\ N_T = \frac{L^2 M_v}{k_g R T_\infty^2}\ ,\ S_r = \exp\left(\frac{\sigma M_v}{d_p R \rho_c T_\infty}\right)$$

$$\beta_M = \frac{1 + Kn_v}{1 + 1.71 Kn_v + 1.333 Kn_v^{\ 2}} \quad \text{and} \tag{13}$$

$$\beta_T = \frac{1 + Kn_g}{1 + 1.71 Kn_g + 1.333 Kn_g^{\ 2}}\ .$$

L is the latent heat of condensation, M_v is the molecular weight of the condensable species, Kn_v is the particle Knudsen number defined as the ratio of the condensable vapour species mean free path to the particle radius, and σ is the surface tension. The mass-transfer part of the Mason equation accounts for the transport of gas molecules by Brownian motion to the surface of a particle. A vapour-phase equilibrium is assumed on the surface of the particle. The Kelvin equation is used to account for the effect of surface curvature. While the above formulation has been shown to work well with species such as water (Wagner, 1982), the exact nature of the behaviour of condensing gas molecules on the particle surface is difficult to model for some other chemical systems. When the condensing species forms a mixture with the other components in the particle, the vapour pressure above the droplet is reduced and condensation can start even before supersaturation and the onset of condensation determined by the deliquescence point of the condensable species. For some species, the assumption of equilibrium at particle surface is not sufficient, but equation 12 has to be supplemented with a mass accommodation coefficient. Such is the case, for instance, if equation 12 is used to represent the growth of particles via crystal growth mechanisms. For many high-temperature systems, an issue to be dealt with is that several physical properties are poorly known. Therefore, any experimental data from a condensation process that can be incorporated in the model equations is valuable. For alkali chloride condensation, this is done using the estimates of Jensen *et al.* (2000) for the diffusion coefficient and the Tolman

length (Paper C). One possible further complication is heterogeneous condensation on agglomerate particles (Rosner and Tandon, 1994). An example of a case where this is a crucial factor is the consideration of the partitioning of trace metals and their subsequent capture efficiency in the electrostatic precipitator.

The time scales of heterogeneous condensation are dependent on the concentrations of particles and particle size distributions. Even more importantly, the rates of heterogeneous condensation are dependent on prevailing temperature-dependent vapour pressures and on their gradients. In usual boiler conditions, various species become supersaturated as the flue gases cool. At the typical number concentrations $1 \cdot 10^7 – 1 \cdot 10^9$ #/cm^3, the simulations indicate that aerosol particles have sufficient scavenging power to prevent high degrees of supersaturation in the main flow during major condensation within the boiler time scales. This is the case when no chemical reactions are involved in condensation processes, for instance, during alkali chloride condensation. Vapour pressure is typically strongly dependent on temperature. Using the extent of saturation vapour pressure variation in the system as a yardstick, the departures from thermodynamic chemical equilibrium, i.e. degrees of supersaturation, are not very large for directly condensing species. Significant departures from thermodynamic equilibrium can arise in the short time scales of the boundary layer (see section 4.3) and when chemical reactions are involved. In addition, after major condensation, the remaining trace amount may be highly supersaturated if saturation vapour pressures are extremely low.

3.4 Particle size dependence of composition

In multi-modal size distributions, different modes usually have different formation mechanisms. In combustion processes, larger mode particles can result from non-volatilised ash-forming fuel components or from re-entrainment from heat exchange surfaces. This accounts for much of the difference in the compositions of the modes. Within the volatilised-condensed mode, the order of condensation reactions determines the distribution of species. The differences in condensation rates determine enrichments in different parts of the mode. If the vapour pressures at particle surfaces were independent of particle size, species that condense later would enrich on the smallest particles. On the other hand, if

the saturation ratio during condensation remains low, the Kelvin effect may reverse this trend and cause these species to enrich on the larger particles of the mode. Particle solidification is an additional consideration. Coagulation and agglomeration act to even out composition differences. The agglomerate shape will increase the surface area available for condensation in larger particles, further evening out the differences. In general, the composition differences within the volatilised-condensed aerosol mode are predicted to be, and have been observed to be, so small that this effect is not usually a major consideration in subsequent studies of deposition (Papers A and B).

3.5 Particle shape evolution during simultaneous agglomeration and sintering

In many systems, it is not sufficient to assume that aerosol particles are spherical. When particles of agglomerate shape are collected or when they deposit on surfaces, it is the size of the primary particles that characterises the material, while much of the information regarding the size distribution of the aggregate particles is lost. Therefore, it is important to consider the dynamics of particle shape evolution. In addition, many qualities of aggregate particles, such as their optical properties, depend on the structure of the particles.

A collision of molten particles results in the formation of a new molten particle, while aggregate particles are generated in the collisions of solid particles (and aggregates). Even if particles are not molten, they can still coalesce after a collision via a number of sintering mechanisms, such as viscous flow, surface diffusion, evaporation-condensation, lattice diffusion, and grain boundary diffusion. In many processes with numerically high particle concentrations, the evolution of particle morphologies is determined by the dynamics of simultaneous agglomeration and sintering. A number of aerosol models have been used for the representation of these phenomena, for instance monodisperse (Kruis *et al.*, 1993), sectional (Xiong and Pratsinis, 1993), self-preserving (Lehtinen, 1997), Monte-Carlo (e.g. Tandon and Rosner, 1999), and moment methods (e.g. Wright *et al.*, 2001). Here the quadrature method of moments is used for the analysis of aerosol particle shape evolution dynamics in a flame reactor.

The shape evolution dynamics can be modelled with a bivariate approach, based on particle volume v_p and excess area e_p (obtained from v_p and a_p) as the state variables. The particle volume remains constant during sintering, while the rate of area reduction can be approximated as being proportional to the excess surface area (Koch and Friedlander, 1990):

$$\frac{da_p}{dt} = -\frac{1}{\tau_f}\left(a_p - a_{sph}\right) = -\frac{1}{\tau_f} e_p \,. \tag{14}$$

Various models depending on the sintering mechanism can be used for τ_f. In a particle collision event, surface area is, like particle volume, thought to be additive, since coalescence is considered separately. Brownian free molecular agglomeration kernel for particles of sizes v_1 and v_2 and excess areas e_1 and e_2 can be calculated based on their collision diameters d_{coll}.

$$\beta\left(v_1, v_2, e_1, e_2\right) = \sqrt{\frac{8\pi k_B T}{\rho_p}} \sqrt{\frac{1}{v_1} + \frac{1}{v_2}} \left(\frac{d_{coll}\left(v_1, e_1\right)}{2} + \frac{d_{coll}\left(v_2, e_2\right)}{2} \right)^2 \tag{15}$$

For the estimation of collision diameters, particles are assumed to possess fractal-like structures. An agglomerate particle that undergoes coalescence can be thought of as being composed of an effective number of spherules (N_S = $(a_p/a_{sph}\,(v_p))^3$) with an effective diameter $d_1 = 6v_p/a_p$. A single spherical particle is composed of one spherule that has the same effective diameter as the particle. A fractal-like agglomerate particle is characterised by a power law:

$$N_{eff} = k_f\left(D_f\right)\left(\frac{d_{gyr}}{d_1}\right)^{D_f}, \tag{16}$$

where k_f is the prefactor, d_{gyr} the gyration diameter of the particle, and D_f its fractal dimension. D_f can be estimated on the basis of v_p and e_p and equation 16 further provides d_{gyr}. If the outer diameter of the agglomerate particle is assumed to approximate the collision diameter, it can be obtained from d_{gyr} as (Rogak *et al.*, 1993):

$$d_{coll} = d_{gyr}\sqrt{\frac{D_f + 2}{D_f}}\,. \tag{17}$$

Figure 5 has the QMOM-based prediction of the mean effective number of spherules per aggregate N_S and comparison against experimental data from a counterflow diffusion flame reactor (Xing, 1997; Xing *et al.*, 1999). Surface diffusion was assumed to be the dominant sintering mechanism. N_S initially increases as a result of agglomeration as the particles are transported from the particle inception plane (PIP) towards the flame. At the flame plane (FLP), there is a marked decrease as a result of sintering. Simulation is conducted until the particle stagnation plane (PSP). Qualitatively, the measured values and predictions are similar, with the location of major sintering predicted correctly. However, on the basis of this graph, it seems that the extent of coagulation that takes place is overpredicted.

The activation energy for sintering by surface diffusion was selected as the fitting parameter in these studies, since its values in the nanoparticle range are poorly known. Particle size and shape evolution dynamics was simulated in two extensively characterised flames. An estimate of the activation energy was obtained from comparisons with experimental data. Too-small activation energy values yield too few spherules per particle and too-early sintering in the flame, while the reverse occurs with too-large activation energy values. Figure 5 visualises the differences in the predictions for the effective number of spherules with three values for activation energies 0.7 GJ/kg-mol, 0.8 GJ/kg-mol (optimum), and 0.9 GJ/kg-mol. With 0.7 GJ/kg-mol, sintering takes place too early and, with 0.9 GJ/kg-mol, sintering does not bring about a major decrease in the number of particles. Looking at the final number of particles, a value slightly greater than 0.8 GJ/kg-mol would seem to be the optimum. However, for cases with the other flame, the optimum is slightly below 0.8 GJ/kg-mol. As a compromise, the value 0.8 GJ/kg-mol was adopted. As the accuracy of the current bivariate QMOM version for this kind of simulation is limited, the current simulations should be considered as of being of an illustrative nature. Further studies are required for more reliable estimates.

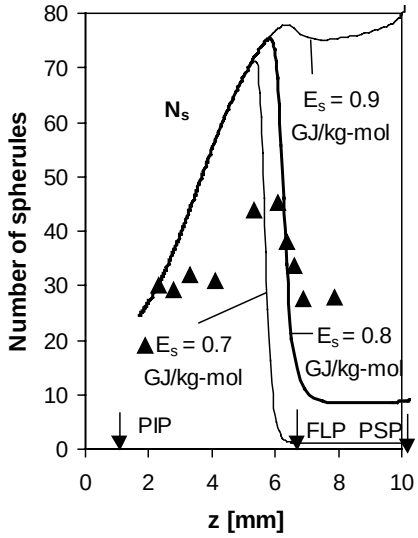

Figure 5. Mean effective number of spherules per aggregate (N_S) with various values of activation energy for sintering by surface diffusion (E_S). Lines represent the simulations and the triangles experimental data (Paper F).

4. Topics in deposit formation

4.1 Particle and vapour co-deposition

The issue of particle and vapour co-deposition couples aerosol dynamics and transport. It is of practical relevance in biofuel combustion, where alkali chlorides are often associated with deposit-related problems. According to the chemical equilibrium, alkali chlorides are thermodynamically expected to be in the vapour phase in the free stream temperatures in the superheaters of typical large-scale combustion boilers, while they are expected to be in the condensed phase on the superheater surfaces. This implies that both direct vapour deposition and boundary layer condensation on aerosol particles and subsequent deposition via thermophoresis are possible. Homogeneous nucleation within the thermal boundary layer and subsequent deposition by thermophoresis and diffusion can also occur. In the literature, these mechanisms are usually stated as possibilities, without further analysis of their relative importance (e.g. Bryers, 1996). Detailed deposition mechanisms are important when determining deposition rates and the physical form of the depositing material. The physical form may have an impact on the subsequent evolution of the properties of the deposit layer.

A number of models that allow for boundary layer condensation on aerosol particles have been presented in the literature. Ahluwalia *et al.* (1986) presented a boundary layer aerosol model aimed at predicting particle and vapour deposition in coal-fired gas turbines. Both homogeneous and heterogeneous nucleation were considered. Castillo and Rosner (1988, 1989) presented a model of deposition on cooled deposition targets in laminar boundary layers that allows for heterogeneous condensation, and the model was subsequently extended to include homogeneous condensation and coagulation as well (e.g. Tandon and Rosner, 1996). The model is applicable to stagnation points. Tandon and Rosner (1996) discussed the importance of including surface roughness in the simulations of particle and vapour co-deposition. Validations with lab-scale experiments have been performed to support the aforementioned studies.

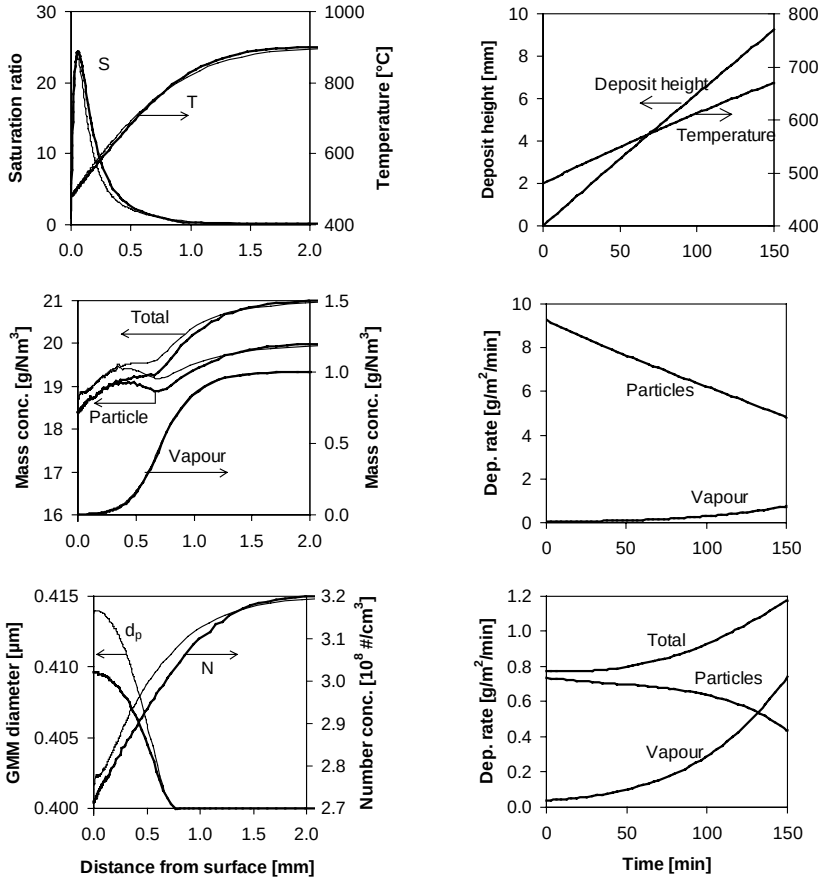

Figure 6. Left: Simulated aerosol properties in thermal boundary layer at the stagnation point of first tube in recovery boiler superheater panel (the stagnation point boundary layer model with bold lines, the CFD-based model with weak lines) Right: Deposit height and temperature (top), total deposition rates (middle), and alkali chloride deposition rates (bottom) as a function of sootblowing cycle time (Paper G).

Paper G presents simulations of alkali chloride deposition on recovery boiler superheater panels. These indicated that the boundary layer processes are indeed significant. Studies with the CFD model indicated that the stagnation point of the first superheater tube is the location that is the most vulnerable to direct vapour deposition. The highest supersaturations of alkali chloride vapours occur there. In the panel section boundary layers, deviations from thermodynamic

equilibrium are predicted to be considerably lower. The chemistry part of the model has been kept simple and only NaCl is considered. Deposit formation is studied during high chloride content liquor combustion (NaCl flue gas concentration 1 g/Nm^3) under typical recovery boiler conditions. A free-stream velocity of 5 m/s and a temperature of 900°C are assumed, while the superheater surface temperature is 480°C. Using the measurements summarised by Mikkanen (2000) as a basis, fume particle concentration in the flue gases is set to 20 g/Nm^3 and the particle sizes are given lognormally distributed, with a geometric mass mean diameter of 0.4 μm and a geometric standard deviation of 1.2, indicative of the primary particle size distribution.

The top left graph in Fig. 6 indicates that the saturation ratio in the stagnation point boundary layer has a maximum value of approximately 24, very close to the surface. The rise in particle concentration visible in the middle left graph indicates the location where major condensation on the particles occurs in the boundary layer. The bottom right graph shows a predicted shift in the deposition mechanisms for alkali chlorides during a recovery boiler soot-blowing cycle. At the beginning, at a superheater surface temperature of 480 °C, alkali chloride deposits mainly in particles, while when the surface temperature of 670 °C is reached at the end of the cycle, vapour and particle deposition are, roughly speaking, equally important. Even if there is a significant shift in the relative importance of vapour and particle deposition, the change in the total deposition rate of alkali chlorides is not as large (increase of 52 %). Homogeneous nucleation is predicted to be insignificant at a fume particle concentration of 20 g/Nm^3. Significant homogeneous nucleation occurs if fume particle concentration is lowered to 1 g/Nm^3.

4.2 Deposition mechanisms in turbulent boundary layers

There are well-established methods for modelling deposition mechanisms in various kinds of boundary layers of particles which are applicable when particle inertia can be neglected (Rosner and de la Mora, 1982; Gökoglu and Rosner, 1984) or it affects particle deposition during transport through a laminar boundary layer (Wessel and Righi, 1988; Konstandopoulos and Rosner, 1995; Brown, 1996). However, when particle sizes are such that the inability of particles to follow turbulent eddies has an effect on deposition rates, the

capabilities of modelling methods become poorer. Both heat and mass transfer correlation-based (e.g. Im and Chung, 1983; Ahluwalia *et al.* 1986; Papers A and B) and computational fluid dynamics- (CFD) based (e.g. Yau and Young (1987); Li *et al.* (1994); Paper C) tools have been used for predicting deposition rates in these cases. It is often sufficient to model deposition without explicit consideration of boundary layer particle concentration profiles. Turbulent impaction rates can be estimated with wall shear stress based correlations. The stopping distance model (Friedlander and Johnstone, 1957; Im and Chung, 1983) provides some sensitivity to interception effects. In non-isothermal cases, the sum of thermophoresis and turbulent impaction provides an initial estimate of the total deposition rate.

Detailed consideration of particle transport in turbulent boundary layers reveals that the mechanisms behind deposition are not simply additive. Buffer layer turbulent eddies fling particles of certain aerodynamic sizes into the laminar sublayer from where they are not carried back in a similar fashion as a result of the absence of significant turbulence. In isothermal flow, this leads to the enrichment of these particles in the laminar sublayer and, if there is thermophoresis present, to intensified deposition by the combined action of inertial transport in turbulent eddies (turbophoresis) and thermophoresis. The correlation and stopping distance models implicitly assume that particles that do not possess enough inertia to reach the surface are instantly carried back to the free stream. Thus, accumulation of particles in the laminar sublayer and interactions with thermophoresis are not considered explicitly. In some cases, this shortcut can distort model predictions.

Paper E presents tests of advanced deposition models embedded in CFD. The model of Guha (1997) provides a framework within which the detailed boundary layer transport mechanisms can be considered. This framework includes a number of approximations for turbulence-averaging the transport terms in equation 1, including the use of the concept of turbulent diffusivity. The inclusion of the Saffman Lift force did not seem necessary, since Guha (1997) obtained equivalent or even slightly better accordance with measurements by not including this effect. Further assuming that $\overline{u}_{gy} = 0$ the turbulence-averaged particle turbophoretic drift velocity in the direction perpendicular to the wall $\overline{u}_{py}$ is given by

$$\overline{u}_{py}\frac{\partial \overline{u}_{py}}{\partial y}+\frac{\overline{u}_{py}}{\tau_p}=-\frac{\partial \overline{u'^2_{py}}}{\partial y}. \qquad (18)$$

Particle mean-square velocity is related to the gas mean-square velocity with the following empirical correlation (Guha, 1997)

$$\overline{u'^2_{py}}\Big/\overline{u'^2_{gy}}=\frac{1}{1+0.7\left(\tau_p/T_L\right)}, \qquad (19)$$

where T_L is the Lagrangian time scale of turbulence. Surface roughness (k_s) is taken into account in the distance from the wall where particle capture is assumed to take place.

Figure 7 presents a reproduction of Guha's (1997) calculations of the dimensionless deposition velocities ($V_{dep}^{+} = J_{dep}/(m_\infty u_*,)$ where J_{dep} is the mass transfer rate of deposition and m_∞ is the free stream concentration) in the experiments of Liu and Agarwal (1974). Liu and Agarwal measured pipe penetrations in isothermal fully developed turbulent flow. The deposition velocities are estimated for quasi-equilibrium conditions, i.e. when the relative (normalised to mean concentration) particle concentration profiles do not change in axial direction and the Saffman lift force is neglected. The right-hand side of the graph shows that the maximum enrichments (defined as the ratio of local particle concentration to free stream concentration) in the boundary layer are obtained at dimensionless relaxation times around 10. With smooth surfaces, maximum enrichments are predicted to be as high as over 400.

In isothermal flow, different combinations of direct free flight to the surface and combined free flight into the laminar sublayer and subsequent diffusion can provide reasonable predictions of observed deposition rates. Paper E demonstrates that model studies of experiments that also involve thermophoresis (Byers, 1967) may provide indirect evidence of the mechanisms behind deposition. A straightforward application of equations 18 and 19 led to a significant over-prediction of deposition rates. This indicates that, in isothermal cases, this formulation places too much emphasis on enrichment-diffusion compared with direct free flight. With thermophoresis, this translates into a marked increase in deposition velocities. Thus, the seemingly good accordance

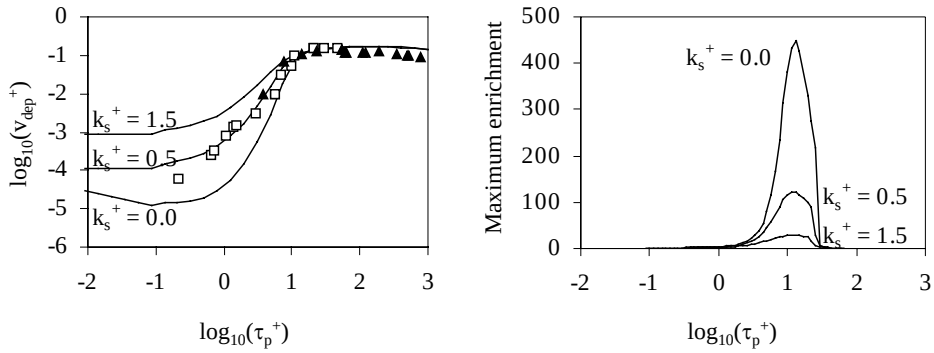

Figure 7. Dimensionless deposition velocities (left) and maximum enrichments (right) as a function of dimensionless particle relaxation time. Simulations with varying dimensionless surface roughnesses (k_s^+) and data of Liu and Agarwal (1974) (paper E).

in Fig. 7 was concluded to be misleading. Based on a literature study, a simplified zero-concentration wall boundary condition, the neglect of the Saffman lift force, and the failure of the model to properly account for the turbulence history of a depositing particle were identified as the deficiencies in the formulation. The first two deficiencies could be remedied with presently available methods, but not the third (Guha, 1997; Young and Leeming, 1997).

Caution should be used with model predictions, such as those in Papers A and B, for particles equally affected by thermophoresis and turbulent impaction even if no excessive interaction effects are expected on the basis of these studies. The tests with Eulerian models for CFD-based analyses demonstrated that, while such models hold promise for the future, at the moment their use requires great care and understanding of the underlying assumptions. For fundamental modelling studies, there is always the option of simulating particle tracks using direct numerical simulation (DNS) (e.g. Brooke *et al.*, 1994; Thakurta *et al.*, 1998).

4.3 Deposit growth and transformations

Deposit-related problems, such as flue gas plugging and corrosion underneath a deposit layer, are very complex and deposition rates, i.e. mass transfer rates from

the flue gases to surfaces, are only a part of the overall phenomenon. The interest in alkali chloride deposition stems from the effects of chlorine species on fouling tendency and their role in chlorine-induced corrosion. Selective chlorine corrosion and accelerated corrosion attack are believed to be caused by the presence of HCl(g) and Cl_2(g) at the metal-deposit interface (see e.g. Grabke *et al*., 1995; Nielsen *et al*., 1999; Nielsen *et al*., 2000; Salmenoja, 2000). Simple models of in-deposit alkali chloride transport and transformations coupled with deposition models provide an opportunity to study the mechanisms behind the generation and transport of HCl(g). HCl(g) is generated as deposited NaCl(c) sulphates with the following reaction:

$$2NaCl(c) + SO_2(g) + 1/2O_2(g) + H_2O(g) \rightarrow Na_2SO_4(c) + 2HCl(g). \qquad (20)$$

Studies of sulphation phenomena and their effects require consideration of deposit growth and temperature profiles during a sootblowing cycle. In calculating deposit growth, perfect sticking for fume particles and vapour has been assumed, while estimates based on industrial observations have been used for coarse particles. Theoretically-based modelling of the contribution of coarse particles on deposit growth is difficult, since it depends on whether coarse particles stick or bounce upon impact or become re-entrained soon afterwards. Temperature profiles for a cylindrical heat exchange tube are obtained from a heat balance (e.g. Senior, 1997).

In the model, the following equation for the condensed NaCl mass concentration z_{NaCl} as a function of the radial co-ordinate r is solved:

$$\frac{\partial z_{NaCl}}{\partial t} = \frac{A}{r}\frac{\partial}{\partial r}\left(\rho_g D_{eff} r \frac{\partial}{\partial r}\left(\frac{v_{eq}}{\rho_g}\right)\right) - \left(\frac{\partial z_{NaCl}}{\partial t}\right)_{sulphation} \qquad (21)$$

where A is the stoichiometric conversion coefficient, D_{eff} is the effective porous medium diffusion coefficient for gas phase transport, and v_{eq} is the equilibrium concentration in the vapour phase. The first term on the-right hand side represents diffusion driven by a chemical potential gradient. Other forms of transport, such as grain boundary diffusion and surface diffusion, also exist and may be significant, but they have not been considered in this study, since not much information concerning them is available.

To gain an idea of the importance of sintering, the magnitude of neck growth due to sintering by evaporation-condensation was estimated for particles 0.4 μm in diameter. NaCl is known to sinter by evaporation-condensation (Kingery and Berg, 1955). Lien *et al.* (1999) suggested, on the basis of their experiments, that this is the most probable sintering mechanism for particles in recovery boiler deposits. The rate of vapour phase sintering is given for the dimensionless neck width *X*, which represents the ratio of neck diameter to particle diameter (Kingery and Berg, 1955):

$$\frac{\partial (X^3)}{\partial t} = \frac{3\sqrt{\pi/2}\,\sigma\, M_v^{3/2}\, p_s\, d_p}{2(RT)^{3/2}\,\rho_c^2}. \qquad (22)$$

Here, since long time scales are involved, Raoult's law is used in the estimation of the saturation vapour pressure p_s.

The kinetics of alkali chloride sulphation is not well known. A two-step rate law, with fast kinetics above the temperature of partial melting and slow kinetics below this temperature, has been assumed here. Fast kinetics is estimated on the basis of the experiments of Iisa *et al.* (1999) and slow on Boonsongsup *et al.* (1997). Figure 8 shows a sudden rise in HCl(g) concentration around 100 min after sootblowing. This arises as the outer surface of the deposits reaches the assumed temperature of partial melting at that moment. Provided that sulphation kinetics for partly molten fume particle is sufficiently rapid, gas phase transport of SO_2 and/or SO_3 limits sulphation. The concentration of SO_2/SO_3, perhaps as short pulses in the widely varying conditions of many combustion processes, seems to be the dominant factor for the presence of high HCl(g) levels in the metal-deposit interface region. The deposition rates of alkali chlorides can have a significant direct effect on sulphation rates only if the SO_2/SO_3 concentrations are sufficiently large. A more important coupling effect may arise via the effect of alkali chlorides on the partial melting of the deposited fume particles.

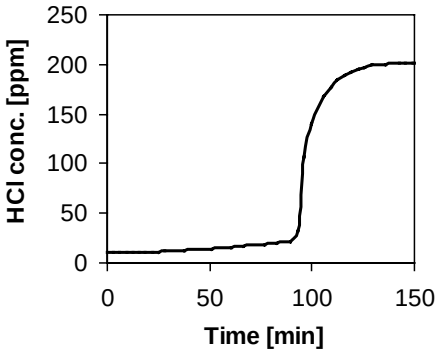

Figure 8. Predicted evolution of HCl concentration in the deposit-metal interface at SO_2 concentration of 100 ppm (Paper G).

The physical form of deposition (particle vs. vapour) may affect the microstructure of the deposits. However, sintering of small fume particles seems to be very rapid within the time scales of recovery boiler superheater sootblowing cycles (Fig. 9). This implies that vapour phase deposits do not necessarily have a much more effective glue effect compared with equivalent fume particle deposits.

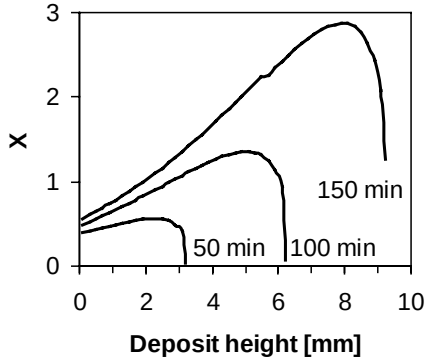

Figure 9. Predictions of the growth of the dimensionless neck width (X) for 0.4 μm particles due to evaporation condensation sintering at various moments during the sootblowing cycle (Paper G).

5. Application to real-world processes

5.1 Recovery boiler

Recovery boilers are used for reprocessing the waste sludge from the paper pulping process, called black liquor (Adams *et al.*, 1998). In addition to recovering the pulping chemicals, recovery boilers also exploit the thermal energy of the residual wood-based material, via combustion, to produce electricity and process steam. An important characteristic of black liquor, regarding resulting fly ash characteristics, is its exceptionally high sodium content, typically about 20% in dry solids. Sodium originates from the pulping chemicals NaOH and Na_2S. Other inorganic elements in black liquor that are important for fly ash chemistry are S, K, and Cl. Black liquor is sprayed into the furnace from a large number of nozzles. Combustion takes place both in the fuel particles and on the char bed on the bottom of the furnace. The char bed is formed from settled fuel particles. Part of the particles, the carryovers, are entrained to the upper furnace. Part of Na, K, S and Cl, volatilises in the furnace.

A significant part of the released inorganic species form condensable species that, later on, during flue gas cooling form a high concentration (10–25 g/Nm^3) of submicron fume particles (Mikkanen *et al.*, 1999a; Mikkanen, 2000). In the superheaters, the mass mean diameter of the fume particles is approximately 0.4 μm. In contrast to many other furnace combustion processes, the volatilised-condensed mode is the main mode of mass. The main chemical component in fume particles is Na_2SO_4. In addition, there are carbonates and chlorides and equivalent potassium species that form an ionic mixture at high temperatures. Before the publication of Paper A, the prevailing theory of fume formation in recovery boilers was based on a reaction-enhanced mechanism, proposed by Cameron (1986, 1987). The theory assumed that initial fume particle formation takes place as sodium vapours that volatilise from the char bed react rapidly to form Na_2CO_3 particles. Later on, these particles were assumed to react with SO_2 and form Na_2SO_4. The deficiency in the theory was that modern furnace temperatures are above the decomposition temperature of Na_2CO_3. Paper A presents an alternative theory, that the first main species to condense is Na_2SO_4. The numerical studies of fume formation presented in Paper A demonstrate the feasibility of the proposed Na_2SO_4-route fume formation mechanisms. At least part of the initial particles originate from volatilised and oxidised metal

impurities. Homogeneous nucleation of Na_2SO_4 may also take place, depending on the kinetics of nucleation and mixing processes in the furnace. It is difficult to know whether a significant number of particles is formed this way, since no measurements of Na_2SO_4 nucleation are available and mixing patterns in the boiler are complex. Moreover, the issue is not of primary interest, since the resulting particle size distributions at the heat exchangers are, to a considerable degree at any rate, determined by coagulation and there is not much variation in fume particle size distribution as a function of operating conditions. Even if all the chemistry-related aspects, such as sulphation kinetics, are not properly known and a 1D representation is approximate, a fairly good accordance between predictions and measured particle size distributions was obtained in the simulations described in Paper A.

The high alkali content and consequent high slagging and fouling propensity of black liquor makes deposit control a significant factor in the design and operation of recovery boilers. Compared with boilers of equal capacity for other fuels, recovery boilers are larger, the maximum steam temperatures are lower, there is more heat exchange surface, and superheater design is more conservative, with wider spacing between the panels of successive tubes. In addition, sootblowing is applied more often. Flue gas plugging and superheater corrosion are still serious intermittent problems. The costs of a recovery boiler shutdown can be remarkable, since the whole pulping process is affected. The mechanisms that lead to the problems are not yet fully understood but, on the basis of electron microscopy studies of deposit layers, fume particles are known to have an important role (e.g. Mikkanen *et al.*, 2001). In Papers A and B, computational simulations were conducted to demonstrate the importance of different deposition mechanisms for vapours, fume particles and various types of coarse particles. The studies spurred the evaluation and further development of the deposition models that were used at that time. Due to the importance of alkali chlorides in chlorine-induced corrosion and fouling phenomena, more detailed studies of alkali chloride deposition mechanisms and rates were carried out (Chapter 4.1, Paper E). It was shown that, with the inclusion of boundary layer phenomena in the models, there is not as much variation in the deposition rates of alkali chlorides in different parts of the superheater section as the uncoupled simulations in Papers A and B suggested. This is in accordance with available probe measurement data (e.g. Adams and Frederick, 1988; Hupa *et al.*, 1998). Simulations of deposit formation and transformations during a

sootblowing cycle were undertaken in order to assess the implications of alkali chloride deposition, especially as concerns deposit sulphation. Deposit sulphation can lead to high HCl concentrations in the metal-deposit region interface entailing a risk of chlorine-induced corrosion. As discussed in Chapter 4.3, the simulations indicate that high SO_2/SO_3 levels seem to be required for high alkali chloride deposition rates to bring about high HCl concentrations. This implies that the use of high-chlorine black liquor does not necessarily cause corrosion problems if boiler operation is able to keep SO_2/SO_3 levels continuously low. Deposition mechanisms for supermicron particles in turbulent boundary layers taken were assessed in Paper F (Chapter 4.2). These are especially important when considering the role of particles re-entrained from superheater deposits in boiler bank fouling. The reliability of the models used in Papers A and B was found to be limited in the case of equally important thermophoresis and turbulent impaction. The deposition rates in the vertical heat exchanger sections (first economiser in A and B, boiler bank in modern designs) for particles in the size range 1–10 μm may actually be higher than our earlier predictions, but it is difficult to estimate by how much. An additional consideration regarding the studies in A and B is that the fully developed channel flow correlations probably led to too-low turbulence levels in the boundary layer (Eskola, 1997; Eskola *et al.*, 1998). These considerations imply that re-deposition of re-entrained particle aggregates from superheaters may be an important consideration. Flue gas path retention measurements, such as those of Lind *et al*. (1999) (for the fluidised bed convection path), could provide some relevant experimental data.

5.2 Bio- and mixed fuel combustion in the fluidised bed

The fluidised bed is a convenient system for the combustion of various kinds of solid fuels, and is able to deal with low-grade fuels that are difficult for other systems. In bio- and mixed fuel combustion in fluidised beds, alkali chlorides and sulphates are often the main species in the fine mode aerosol particles. Therefore, much of the discussion related to recovery boilers is also applicable to the convection paths of fluidised beds, especially concerning fouling and corrosion problems. As a difference, the fine mode concentrations are significantly lower and the coarse particles form the main mode on a mass basis. A predicted difference in alkali chloride deposition mechanisms is that, unlike in

recovery boilers, homogeneous nucleation inside the thermal boundary layer is predicted to be significant and, thus, to determine the deposition rates of alkali chlorides (Paper E). This is due to the less effective scavenging power of the smaller fine mode particle concentration. As nucleation takes place close to the surface, alkali chloride deposition velocities are significantly higher than in recovery boilers.

5.3 Pulverised coal combustion

Pulverised coal combustion is one of the most widely used techniques to generate energy in a large-scale unit. Therefore, problems related to deposit formation have been widely studied worldwide. Slagging of the furnace walls or the superheater surfaces can occasionally be a severe problem. In pulverised coal-fired boilers, the main mass mode of fly ash is formed from the mineral impurities in coal that are either remnants of coal particles when the char has burned away or extraneous mineral particles that have been liberated in the coal grinding process and entered the furnace as such. Paper C presents a CFD-based scheme intended for the prediction of the effect of the flow fields on slagging. The scheme deals with the two slagging mechanisms that were deemed to be the most significant. The first is slagging as a result of simultaneous high temperature and particle deposition fluxes. This can lead to high temperatures within the deposits, causing them to sinter to levels of difficult removability within the time scale of a sootblowing cycle. The second is fast deposit growth resulting from the deposition of sticky pyrite-derived particles that have not had time to fully oxidise and crystallise. This mechanism can be important in the burner belt region. The computational scheme couples particle trajectories, deposition fluxes, heat fluxes, and deposit sintering dynamics. Particle trajectories are solved with standard methods the commercial CFD codes (here Fluent) provide. Pyrite conversion kinetics and iron oxidation kinetics are solved along the trajectories. Particle trajectories provide estimates of inertial impaction rates on furnace walls and the concentrations in the CFD grid cells next to a wall. Deposition rates by turbulent impaction are determined based on these concentrations and deposition velocities obtained from wall shear stress-based correlations. Deposition velocities are calculated for inertial impaction on superheater tubes with correlations by Wessel and Righi (1988). Figure 10 presents a prediction of deposition velocities on furnace walls. Particle sticking

is estimated with a commonly used model that is based on ash particle viscosities (Walsh *et al.*, 1990). The CFD code provides the radiative heat flux and the (less significant) convective heat flux on the walls, while correlations can predict convective heat flux on the superheater tubes, using local flow conditions as the starting point. Heat flux calculation was incorporated in the scheme after Paper C, using Senior's model (1997) in a similar manner as in the alkali chloride simulations (chapter 4.3). Following Senior, estimates of the time scales of sintering in the maximum deposit temperature that are reached during a time scale of 8 hours in different parts of the boiler are used as indications of slagging propensities. Typical problematic coal fly ash size and property distribution can be used as the starting point for calculations. The scheme also includes a rudimentary model for the incorporation of CCSEM data, but it is very difficult to get reliable coal-specific predictions. The most easily attainable information of practical relevance is probably the abundance of large (> 50 μm in diameter) pyrite mineral inclusions.

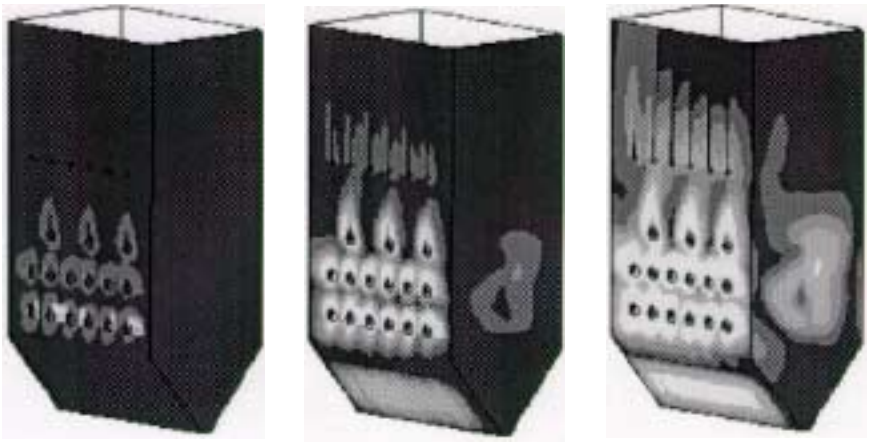

Figure 10. Predictions of turbulent impaction velocities for 10 μm (left), 50 μm (middle) and 100 μm (right) particles in an industrial furnace. Dark < 2 mm/s < Dark grey < 5 mm/s < Grey < 1 cm/s < Light grey < 2 cm/s < Light (paper C).

5.4 Medium-speed diesel engine

Medium-speed diesel engines are frequently used in marine and land-based power generation applications. The advantage of diesel engines is their ability to burn low-grade heavy fuel oils. Because of the high content of impurities in low-grade fuels, there can be a relatively high content of submicron particulate ash formed via volatilisation-condensation processes. This, associated with the corrosive nature of the impurities, has led to occasional exhaust valve failures. Modelling studies of particle formation and deposition in diesel engines were carried out and reported in Paper B. The studies served as an introduction to aerosol issues in medium-speed diesel engines and provided initial estimates of deposition mechanisms. Because of the high velocities at the valve, turbulent inertial effects can be important even in the submicron range. However, the magnitude of deposition velocities does not seem to be a very important consideration with regard to valve failures, since the rates at which particles are transported to the surface are rather high throughout the particle size distribution spectrum. This implies that issues related to particle sticking and re-entrainment are more important. Subsequent experimental studies have concentrated more on aerosol characterisation and the chemical aspects of deposit-metal interaction (e.g. Lyyränen *et al*., 1999).

5.5 Behaviour of revaporised material in severe nuclear accidents

One of the initial motivations for the simulation of aerosol formation dynamics on laminar flow reactors was interest in the behaviour of revaporised material in severe nuclear accidents. Severe nuclear accident scenarios that do not involve an immediate failure of the containment building usually assume that approximately 80% of the fission products released from the reactor core deposit on the surfaces of the primary coolant circuit. Due to the decay heat of the radionuclides, deposited species, such as those of caesium, may vaporise at a later stage. Their fate is an essential consideration for an accident scenario that involves a containment failure after these species have revaporised. Revaporisation is usually assumed to occur during a slow laminar flow towards the cooler parts of the primary circuit. Therefore, revaporised species may

nucleate and form new aerosol particles. The computer models that are used to simulate nuclear accidents usually treat aerosol particles by assuming them to be of constant size (e.g. 0.1 μm) (e.g. Heames *et al*., 1992). However, in the case of revaporisation, it is imaginable that, due to slow flow rates, nucleation rates are limited and low particle number concentrations are generated. This implies a possibility that the number concentrations are so low that the generated particles can grow to the supermicron size range via heterogeneous condensation. A series of experiments with CsOH was performed to test this hypothesis (Valmari *et al*., 1998). The experiments revealed that CsOH nucleates very vigorously, even in the presence of a 10^7 #/cm^3 seed particle concentration. This means that the hypothesis of particle growth to the supermicron range is not very probable and detailed studies with a view to the estimation of CsOH nucleation kinetics were not warranted.

6. Conclusions

In this thesis, computational methods for simulating aerosol dynamics and transport have been developed. Two different versions of the sectional aerosol model were coupled with a CFD code. One is a full Eulerian model and the other is a boundary layer-type streamtube model. Computational requirements limit the use of the full Eulerian model. Indeed, in cases where it was applied in this work, alternative models were deemed to be more appropriate. This demonstrates that the development of a universal CFD-based aerosol model is difficult. Instead, it is often more appropriate to make suitable simplifying assumptions, such as a parabolic flow, a constant size distribution shape or a reduction to one dimension. Here, suitable assumptions allowed the use of computationally efficient and accurate methods. In the simulation of aerosol formation dynamics in a laminar flow reactor, the streamtube-based sectional model was able to provide an accurate solution of the model equations within a reasonable computing time. A method of coupled moving and fixed grids was used to minimise numerical errors and enhance computational efficiency. For boundary layers, the streamtube model made possible a rigorous analysis of non-isothermal pipe flow experiments. In the cases of the stagnation point boundary layer and the counterflow diffusion flame reactor, it was appropriate to reduce the flow description to one dimension, and thus, focus the computational resources on aerosol transport and dynamics studies. The bivariate quadrature method of moments (QMOM) was able to provide a reasonable computational representation of simultaneous agglomeration sintering processes in a flame reactor. However, further work is still required to make the method more accurate for bivariate studies.

Computational predictions of aerosol formation were carried out. For the recovery boiler, these demonstrated the feasibility of Na_2SO_4-route fume formation mechanism theory. There is experimental data that agrees with the model predictions to support the proposed theory. The simulations do not provide a clear answer to the question of whether homogeneous nucleation of Na_2SO_4 is important or whether the majority of fume particles are formed by the nucleation of impurity metals. However, as far as the resulting particle size distribution is concerned, this is not of primary importance. There is not much variation in the size distributions as a function of operating conditions, since agglomeration evens out, to a significant degree, the differences that may arise

in the early stages of formation. In addition, deposition rates are not sensitive to particle size in the submicron size range. After initial fume particle formation, gas-to-particle conversion rates seem to be fast enough to prevent large supersaturations in the free stream until only trace concentrations of the condensable species exist. Rather, it is the kinetics of reactions, especially that of sulphation, that may cause deviations from thermodynamic equilibrium.

Differences in deposition rates for different particle modes and vapours are an important consideration in the analysis of deposit-related problems, such as fouling, slagging and corrosion. An issue where aerosol dynamics and transport are especially significant is the case of alkali chloride deposition. There seems to be a great deal of variation in the importances of particle and vapour deposition in the typical temperature range of biofuel-fired boiler superheater surfaces. In recovery boilers, particle deposition is the dominant final mechanism on freshly soot-blown superheater surfaces, while direct vapour deposition can be equally important at higher deposit layer surface temperatures. While the mechanisms vary, the total deposition rates of alkali chlorides do not change as much. Homogeneous nucleation is predicted to be negligible in recovery boiler superheater tube boundary layers, but the reverse is true for conditions resembling fluidised beds during bio- and mixed fuel combustion.

Simulations of deposit transformations provide some ideas of the implications of alkali chloride deposition. No large effects are expected for sintering properties, whereas predictions for the effects on HCl generation and subsequent chlorine-induced corrosion are dependent on the assumptions regarding the kinetics of sulphation. At any rate, by providing estimates of the deposit layer composition, the model opens a pathway for experimental validation. As another issue regarding deposit formation, the coupling between thermophoresis and turbulent impaction was studied. There is probably some degree of coupling that increases deposition velocities, though the magnitude of this effect was not determined. It was noted that, as a result of the complex nature of the interactions involved, simplifications and an insufficient physical basis in some turbulent impaction models, such as the stopping distance model, hamper their predictive capabilities in nonisothermal cases. Computational fluid dynamics-based models can provide indications of the effect of operating conditions on deposit formation, while the analysis of the effects of surface geometry details is difficult. The generally-known guideline for operation and design is that flows and heat fluxes should be

distributed as evenly as possible over the active heat exchange area. Overall, it should be remembered that deposit formation is a complicated issue and the results of the deposition studies of this research only provide some pieces for the overall puzzle.

As a whole, the work carried out in this thesis has provided modelling tools for the analysis of aerosol formation and deposition mechanisms in various industrial systems. It was deemed better to apply specific models to specific cases rather than aim for a comprehensive global model. This way, the level of detail and accuracy can be adjusted based on the needs of each particular study. The methods developed in this research provide novel computationally efficient alternatives to the array of existing options. While the application studies demonstrate the ability of the models to provide a detailed understanding of key aerosol issues in various processes, there is still a lot of scope for future research and development, for instance in extending the coverage of chemistry-related aspects and improving the coupling with experimental research.

References

Adams, T. and Frederick, W. J. (1988) *Kraft recovery boiler physical and chemical processes*. American Paper Institute. New York.

Adams, T., Frederick, W. J., Grace, T. Hupa, M., Iisa, K., Jones A. and Tran, H. (1998) *Kraft Recovery Boilers*. Tappi Press, Atlanta.

Ahluwalia, R., Im, K., Chuang, C. and Hajduk J. (1986) Particle and vapor deposition in coal-fired gas turbines. Proceedings of the 31st Int'l Gas Turbine Conference, Düsseldorf, West Germany, Available also as ASME report 86-GT-239.

Anderson, A. and Debnath, N. (1983) Reaction of NaCl(s) with SO_2(g) and O_2(g) to form Na_2SO_4(s). A charge-transfer reaction. *J. Phys. Chem.* **87**, 1938–1941.

Boonsongsup, L. Iisa, K. and Frederick, W. J. (1997) Kinetics of the sulfation of NaCl at combustion conditions. *Ind. Eng. Chem. Res*. **36**, 4212–4216.

Brooke, J., Hanratty, T. and McLaughlin, J. (1994) Free flight mixing and deposition of aerosols. *Phys. Fluids* **6**, 3404–3415.

Brown, D. (1996) Development of a three-dimensional coupled flow, species and aerosol model: Applications to particle deposition in gas turbines and aerosol formation and growth in jet engine exhausts. PhD Dissertation, University of Cincinnati.

Brown, D., Pyykönen, J. and Jokiniemi, J. (1998) Comparison of lognormal moment and sectional representations of aerosol dynamics processes. *J. Aerosol Sci.* **29**, Suppl. 1, 85–86.

Bryers, R. (1996) Fireside slagging, fouling and high-temperature corrosion of heat transfer surfaces due to impurities in steam-raising fuels. *Prog. Energy Combust. Sci.* **22**, 29–120.

Byers, R. (1967) Particle deposition from turbulent streams by means of thermal force. Ph. D. Thesis, The Pennsylvania State University.

Cameron, J. (1986) Fume generation in kraft recovery boilers. PIMA March 1986. 32–34.

Cameron, J. (1987) Reaction enhanced vaporisation of molten salt. *Chem. Eng. Comm.* **59**, 243–257.

Castillo, J. and Rosner, D. (1988) Nonequilibrium theory of surface deposition from particle-laden, dilute condensible vapor-containing stream, allowing for particle thermophoresis and vapor scavenging within the laminar boundary layer. *Int. J. Multiphase Flow* **14**, 99–120.

Castillo, J. and Rosner, D. (1989) Theory of surface deposition from a unary dilute vapor-containing stream allowing for condensation within the laminar boundary layer. *Chem. Eng. Sci.* **44**, 925–937.

Christensen, K. (1995) The formation of submicron particles from the combustion of straw. PhD Thesis, Technical University of Denmark.

Christensen, K., Stenholm, M. and Livbjerg, H. (1998) The formation of submicron aerosol particles, HCl and SO_2 in straw-fired boilers. *J. Aerosol Sci.* **29**, 421–444.

Couch, G. (1994) Understanding slagging and fouling in pf combustion. IEA Coal Research, London.

Eskola, A. (1997) Deposition of aerosol particles and alkali vapours on heat exchanger surfaces. Master's thesis. Helsinki University of Technology. (in Finnish).

Eskola, A. Jokiniemi, J. Lehtinen, K. and Vakkilainen, E. (1998) Modelling alkali salt deposition on kraft recovery boiler heat exchangers in the superheater section. Proceedings of the 1998 International Chemical Recovery Conference. 469-486.

Fluent Inc. (1996) Fluent user's guide, Release 4.4.

Frenkel, J. (1955) *Kinetic theory of liquids*. Dover, New York.

Friedlander, S. (2000) *Smoke, dust and haze: fundamentals of aerosol dynamics*. Second Edition. Oxford University Press, New York.

Friedlander, S. and Johnstone, H. (1957) Deposition of suspended particles from turbulent gas streams, *Ind. Eng. Chem*. **49**, 1151–1156.

Fuchs, N. (1964) *The mechanics of aerosols*. Pergamon, New York.

Garrick, S., Zachariah, M. and Lehtinen, K. (2001) Modeling and simulation of nanoparticle coagulation in a high Reynolds number incompressible flows. Proceeding of the National Conference of the Combustion Institute, March 25–27, Oakland.

Gelbard, F. (1990) Modeling multicomponent aerosol particle growth by vapor condensation. *Aerosol Sci. Tech.* **12**, 399–412.

Gelbard, F., Tambour, Y. and Seinfeld, J. (1980) Sectional representations for simulating aerosol dynamics. *J. Colloid Int. Sci.* **76**, 541–556.

Girshick, S. and Chiu C.-P. (1990) Kinetic nucleation theory: A new expression for the rate of homogeneous nucleation from an ideal supersaturated vapor. *J. Chem. Phys.* **93**, 1273–1277.

Grabke, H., Reese, E. and Spiegel, M. (1995) The effects of chlorides, hydrogen chloride, and sulfur dioxide in the oxidation of steels below deposits. *Corrosion Science* **37**, 1023–1043.

Guha, A. (1997) A unified Eulerian theory of turbulent deposition to smooth and rough surfaces. *J. Aerosol Sci*. **28**, 1517–1537.

Gökoglu, S. and Rosner, D. (1984) Correlation of thermophoretically-modified small particle diffusional deposition rates in forced convection systems with

variable properties, transpiration cooling and/or viscous dissipation. *Int J. Heat Mass Transfer* **27**, 639–646.

Haynes, B., Jander, H., Mätzing, H. and Wagner H. (1981) The influence of various metals on carbon formation in various flames. *Combustion and Flame* **40**, 101–103.

Heames, T., Williams, D., Bixler, N., Grimley, A., Wheatley, C., Johns, N., Domagala, P., Dickson, L., Alexander, C., Osborn-Lee, I., Zawadzki, S., Rest, J., Mason, A. and Lee, R. (1992) VICTORIA: a mechanistic model of radionuclide behavior in the reactor coolant system under sever accident conditions. USNRC/Sandia National Laboratories Report NUREG/CR-5545 / SAND90-0756, Rev. 1.

Hupa, M., Backman, R. Skrifvars B. and Forssén, M. (1998) Liquor-to-liquor differences in combustion and gasification processes: dust composition and melting properties. Proceedings of the 1998 International Chemical Recovery Conference. 615–628.

Iisa, K., Lu, Y. and Salmenoja, K. (1999) Sulfation of potassium chloride at combustion conditions. *Energy & Fuels* **13**, 1184–1190.

Im, K. and Chung, P. (1983) Particulate deposition from turbulent parallel streams. *AIChE J.* **29**, 498–505.

Jacobson, M. and Turco, R. (1995) Simulating condensational growth, evaporation, and coagulation of aerosols using a combined moving and stationary grid. *Aerosol Sci. Tech.* **22**, 73–92.

Jensen, J. Nielsen, L. Schultz-Møller, C. Wedel, S. and Livbjerg, H. (2000) The nucleation of aerosols in flue gases with a high content of alkali - a laboratory study. *Aerosol Sci. Tech.* **33**, 490–509.

Jokiniemi, J., Lazaridis, M., Lehtinen, K. and Kauppinen E. (1994) Numerical simulation of vapour-aerosol dynamics in combustion processes. *J. Aerosol Sci.* **25**, 429–446.

Kingery, W. and Berg, M. (1955) Study of the initial stages of sintering solids by viscous flow, evaporation-condensation, and self-diffusion. *J. App. Phys.* **26**, 1205–1212.

Koch, W. and Friedlander, S. (1990) The effect of particle surface coalescence on the surface area of a coagulating aerosol, *J. Coll. Interface Sci.* **140**, 419–427.

Konstandopoulos, A. and Rosner, D. (1995) Inertial effects on thermophoretic transport of small particles to walls with streamwise curvature, I. Theory. *Int J. Heat Mass Transfer* **38**, 2305–2315.

Kruis, F., Kusters, K., Pratsinis, S. and Scarlett, B. (1993) A simple model for the characteristics of aggregate particles undergoing coagulation and sintering. *Aerosol Sci. Technol.* **19**, 514–526.

Kumar, S. and Ramkrishna, D. (1997) On the solution of population balance equations by discretization-III. Nucleation, growth and aggregation of particles. *Chem. Eng. Sci*. **52**, 4659–4679.

Lehtinen, K. (1997) Theoretical studies on aerosol agglomeration processes. VTT Publications 304. Academic dissertation. 45 p. + app. 89 p.

Li, A., Ahmadi, G., Bayer, R. and Gaynes, M. (1994) Aerosol particle deposition in an obstructed turbulent duct flow. *J. Aerosol Sci.* **1**, 91–112.

Lien, S. Frederick, J.W., Ling, A. and Tran, H. (1999) Sintering and densification rates for recovery boiler fume deposits. TAPPI Engineering Conference Proceedings, Anaheim, (1999).

Lind, T., Kauppinen, E., Sfiris, G., Nilsson, K. and Maenhaut, W. (1999) Fly ash deposition onto the convective heat exchangers during combustion of willow in circulating fluidized bed boiler. In: *Impact of Mineral Impurities in Solid Fuel Combustion.* Eds. Gupta, T., Wall, T. and Baxter, L. (Kluwer Academic / Plenum Publishers, New York), 541–553.

Liu, B. and Agarwal, J. (1974) Experimental observation of aerosol deposition in turbulent flow. *J. Aerosol Sci*. **5**, 145–155.

Lyyränen, J., Jokiniemi, J., Kauppinen, E. and Joutsensaari, J. (1999) Aerosol characterisation in medium-speed Diesel engines operating with heavy fuel oils. *J. Aerosol Sci.* **30**, 771–784.

Mackowski, D., Tassopoulos , M. and Rosner, D. (1994) Effect of radiative heat transfer on coagulation dynamics of combustion-generated particles. *Aerosol Sci. Technol.* **20**, 83–99.

Mason, B. (1957) *The physics of clouds*, 1st Edition. Clarendon Press, Oxford.

McGraw, R. (1997) Description of aerosol dynamics by the quadrature method of moments. *Aerosol Sci. Technol.* **27**, 155–265.

Mikkanen, P. (2000) Fly ash particle formation in kraft recovery boilers. VTT Publications 421. Academic dissertation. 69 p. + app. 116 p.

Mikkanen, P., Kauppinen, E., Pyykönen, J., Jokiniemi, J., Aurela, M., Vakkilainen E. and Janka, K. (1999a) Alkali salt ash formation in four Finnish industrial boilers. *Energy & Fuels* **13**, 778–795.

Mikkanen, P., Jokiniemi, J., Kauppinen, E. and Vakkilainen, E. (2001) Deposit formation study at an operating recovery boiler. Submitted for publication in *Fuel Process. Technol.*

Mikkanen, P., Pyykönen, J. and Jokiniemi, J. (1999b) NaOH and NaCl sulphation in recovery boiler flue gas conditions. Technical Research Centre of Finland, Espoo. VTT Chemical Technology Research report KET839/99.

Mordy, W. (1959) Computations of the growth by condensation of a population of cloud droplets. *Tellus* **11**, 16–44.

Murata, K., Carrol, D., Washington, K., Gelbard, F., Valdez, G., Williams, D. and Bergeron, K. (1989) User's manual for CONTAIN 1.1: A computer code for severe nuclear reactor accident containment analysis. Sandia National laboratories, NUREG/CR-5026.

Nguyen, H., Okuyama, K., Mimura, T., Kousaka, Y., Flagan, R. and Seinfeld, J. (1987) Homogeneous and heterogeneous nucleation in a laminar flow reactor. *J. Colloid Interface Sci.* **119**, 491–504.

Nielsen, H., Frandsen, F. and Dam-Johansen, K. (1999) Lab-scale investigations of high-temperature corrosion phenomena in straw-fired boilers. *Energy & Fuels* **13**, 1114–1121.

Nielsen, H., Frandsen, F., Dam-Johansen, K. and Baxter, L. (2000) The implications of chlorine-associated corrosion on the operation of biomass-fired boilers. *Prog. Energy and Comb. Sci.* **26**, 283–298.

Raes, F. and Janssens, A. (1986) Ion-induced aerosol formation in a H_2O-H_2SO_4 system - II. Numerical calculations and conclusions. *J. Aerosol Sci.* **17**, 715–722.

Ramkrishna, D. (2000) *Population balances: theory and applications to particulate systems in engineering.* Academic Press, San Diego.

Rogak, S., Flagan, R. and Nguyen, H. (1993) The mobility and structure of aerosol agglomerates. *Aerosol Sci. Technol.* **18**, 25–47.

Rosner, D. and de la Mora, J. (1982) Small particle transport across turbulent nonisothermal boundary layers. *J. Eng. Power* **104**, 885–894.

Rosner, D. and Tandon, P. (1994) Prediction and correlation of accessible area of large multiparticle aggregates. *AIChE J.* **40**, 1167–1182.

Rosner, D. and Yu, S. (2001) Monte-Carlo simulation of free-molecule regime Brownian aggregation and simultaneous spheroidization. *AIChE J.* **47**, 545–561.

Salmenoja, K. (2000) Field and laboratory studies on chlorine-induced superheater corrosion in boilers fired with biofuels, PhD Thesis, Åbo Akademi Report 00-1, 2000.

Seigneur, C., Hudischewskyj, A., Seinfeld, J., Whitby, K., Whitby, E., Brock, J. and Barnes, H. (1986) Simulation of aerosol dynamics: A comparative review of mathematical models. *Aerosol Sci. Tech.* **5**, 205–222.

Senior, C. (1997) Predicting removal of coal ash deposits in convective heat exchangers. *Energy & Fuels* **11**, 416–420.

Sher, R. and Jokiniemi, J. (1993) NAUAHYGROS 1.0: A code for calculating the behavior of aerosols in nuclear power plant containments following a severe accident. EPRI TR-102775.

Simonsen, O. and Livbjerg, H. (1992) The influence of seed nuclei on aerosol condensation. *Comp. and Chem. Eng.* **16**. Suppl., 279–387.

Steinberg, M. and Schofield, K. (1990) The chemistry of sodium with sulphur in flames. *Prog. Energy Combust. Sci.* **16**, 311–317.

Sutugin, A. and Fuchs, N. (1970) Formation of condensation aerosols under rapidly changing environmental conditions. *Aerosol Sci.* **1**, 287–293.

Tandon, P. and Rosner, D. (1996) Codeposition on hot CVD surfaces: Particle dynamics and deposition roughness interactions. *AIChE J.* **42**, 1673–1684.

Tandon, P. and Rosner, D. (1999) Monte Carlo simulation of particle aggregation and simultaneous restructuring. *J. Coll. Interface Sci.* **213**, 273–286.

Thakurta, D., Chen, M., McLaughlin, J. and Kontomaris, K. (1998) Thermophoretic deposition of small particles in a direct numerical simulation of turbulent channel flow. *Int. J. Heat Mass Transfer*. **41**, 4167–4182.

Wagner, P. (1982) Aerosol growth by condensation. In: *Topics in Current Physics, Aerosol Microphysics II* (Edited by Marlow, W.), Springer-Verlag, Berlin, 129–178.

Valmari, T., Pyykönen, J., Brown, D., Jokiniemi, J. and Kauppinen, E. (1998) CsOH aerosol formation and growth in laminar flow. In: *Nuclear Aerosols in*

Reactor Safety. Proceedings of an OECD/CSNI Workshop 15-18 June Cologne. NEA/CSNI/R(98)4, GRS-166.

Walsh, P., Sayre, A., Loehden, D., Monroe, D., Beér, J. and Sarofim, A. (1990) Deposition of bituminous coal ash on an isolated heat exchanger tube: effects of coal properties on deposit growth. *Prog. Energy Combust. Sci* **16**, 327–345.

Wessel, R. and Righi, J. (1988) Generalized correlations for inertial impaction of particles on a circular cylinder. *Aerosol Sci. Technol.* **9**, 29–60.

Whitby, E. and Hoshino, M. (1996) Particle size distribution in a low pressure SiH_4:O_2:He chemical vapor deposition, reactor experimental and numerical results. *J. Electrochem. Soc.* **143**, 3397–3404.

Whitby, E. and McMurry, P. (1997) Modal aerosol dynamics modeling. *Aerosol Sci. Tech.* **27**, 673–688.

Wilck, M., Hämeri, K., Stratmann, F. and Kulmala, M. (1998) Determination of homogeneous nucleation rates from laminar-flow diffusion chamber data. *J. Aerosol Sci.* **29**, 899–911.

Wilck, M. and Stratmann, F. (1997) A 2-D multicomponent modal aerosol model and its application to laminar flow reactors. *J. Aerosol Sci.* **28**, 959–972.

Wright, D. (2000) Retrieval of optical properties of atmospheric aerosols from moments of the particle size distribution. *J. Aerosol Sci.* **31**, 1–18.

Wright, D., McGraw, R. and Rosner D. (2001) Bivariate extension of the quadrature method of moments for modeling simultaneous coagulation and sintering of particle populations. *J. Coll. Interface Sci.* **236**, 242–251.

Wu, J. and Menon, S. (2000) Aerosol dynamics in the near-field of engine exhaust plumes. *Journal of Applied Meteorology* **40**, 795–809.

Xing, Y. (1997) Synthesis and morphological evolution of inorganic nanoparticles in gas phase flames. Dissertation, Yale University.

Xing, Y., Köylü, Ü. and Rosner D. (1996) Synthesis and restructuring of inorganic nano-particles in counterflow diffusion flames. *Combustion and Flame* **107**, 85–102.

Xing, Y., Köylü, Ü. and Rosner D. (1999) In situ light-scattering measurements of morphologically evolving flame-synthesized oxide nanoaggregates. *Applied Optics* **38**, 2686–2697.

Xiong, Y. and Pratsinis, S. (1993) Formation of agglomerate particles by coagulation and sintering – Part I. A two-dimensional solution of the population balance equation. *J. Aerosol Sci.* **24**, 282–300.

Yau, K. and Young, J. (1987) The deposition of fog droplets on steam turbine blades by turbulent diffusion. *J. Turbomachinery* **109**, 429–435.

Young, J. (1992) Two-dimensional, nonequilibrium wet-steam calculations for nozzles and turbine cascades. *J. Turbomachinery* **114**, 569–579.

Young, J. and Leeming, A. (1997) A theory of particle deposition in turbulent pipe flow. *J. Fluid. Mech.* **340**, 129–159.

Appendices of this publication are not included in the PDF version.
Please order the printed version to get the complete publication
(http://otatrip.hut.fi/vtt/jure/index.html)

Published by

Vuorimiehentie 5, P.O.Box 2000, FIN–02044 VTT, Finland
Phone internat. +358 9 4561
Fax +358 9 456 4374

Series title, number and report code of publication

VTT Publications 461
VTT–PUBS–461

Author(s)
Pyykönen, Jouni

Title

Computational simulation of aerosol behaviour

Abstract

Computational methods have been developed for the simulation of aerosol dynamics and transport. Coupled aerosol-computational fluid dynamics (CFD) models are presented. A boundary layer type sectional model is shown to be able to provide an accurate solution of aerosol formation dynamics equations in a laminar flow reactor within a reasonable computing time. A bivariate extension of the quadrature method of moments (QMOM) is also discussed. The models have been applied to combustion processes. Computational simulations with a one-dimensional sectional model demonstrate the feasibility of the Na_2SO_4-route fume formation mechanism theory for recovery boilers. Estimates of deposition velocities are obtained for particles of various sizes and inorganic vapours, and for various conditions. It is noted that aerosol dynamics and transport significantly affect alkali chloride deposition. There seems to be a great deal of variation in the proportions of alkali chloride particle and vapour deposition in the typical range of biofuel-fired boiler superheater conditions.

Keywords

aerosols, aerosol formation, deposition, modelling, population balances, computational fluid dynamics, laminar flow reactors, combustion processes, fly ash, recovery boilers, boundary layers

Activity unit

VTT Processes, Biologinkuja 7, P.O.Box 1401, FIN-02044 VTT, Finland

ISBN	Project number
951–38–5977–0 (soft back ed.) 951–38–5978–9 (URL:http://www.inf.vtt.fi/pdf/)	KETT921

Date	Language	Pages	Price
March 2002	English	70 p. + app. 154 p.	E

Name of project	Commissioned by

Series title and ISSN	Sold by
VTT Publications 1235–0621 (soft back ed.) 1455–0849 (URL: http://www.inf.vtt.fi/pdf/)	VTT Information Service P.O.Box 2000, FIN-02044 VTT, Finland Phone internat. +358 9 456 4404 Fax +358 9 456 4374

Computational methods have been developed for the simulation of aerosol dynamics and transport. One-dimensional aerosol models and coupled aerosol-computational fluid dynamics (CFD) models are presented. These are applied to simulations of aerosol formation and deposition in various processes. Closer consideration is given to aerosol formation dynamics in laminar flow reactors and in combustion processes. The deposition of alkali chlorides is predicted to be significantly affected by boundary layer aerosol dynamics. There seems to be a great deal of variation in the proportions of alkali chloride particle and vapour deposition in the typical range of biofuel-fired boiler superheater conditions.

Tätä julkaisua myy
VTT TIETOPALVELU
PL 2000
02044 VTT
Puh. (09) 456 4404
Faksi (09) 456 4374

Denna publikation säljs av
VTT INFORMATIONSTJÄNST
PB 2000
02044 VTT
Tel. (09) 456 4404
Fax (09) 456 4374

This publication is available from
VTT INFORMATION SERVICE
P.O.Box 2000
FIN–02044 VTT, Finland
Phone internat. + 358 9 456 4404
Fax + 358 9 456 4374

ISBN 951–38–5977–0 (soft back ed.)
ISSN 1235–0621 (soft back ed.)

ISBN 951–38–5978–9 (URL: http://www.inf.vtt.fi/pdf/)
ISSN 1455–0849 (URL: http://www.inf.vtt.fi/pdf/)